(12) INTERNATIONAL APPLICATION PUBLISHED UNDER THE PATENT COOPERATION TREATY (PCT)

(19) World Intellectual Property Organization
International Bureau

(43) International Publication Date
19 March 2020 (19.03.2020)

WIPO | PCT

(10) International Publication Number
WO 2020/053423 A1

(51) International Patent Classification:
H01M 10/054 (2010.01) *H01M 10/0562* (2010.01)

(21) International Application Number:
PCT/EP2019/074557

(22) International Filing Date:
13 September 2019 (13.09.2019)

(25) Filing Language: English

(26) Publication Language: English

(30) Priority Data:
18194653.4 14 September 2018 (14.09.2018) EP

(71) Applicant: **AARHUS UNIVERSITET** [DK/DK]; Nordre Ringgade 1, 8000 Aarhus C (DK).

(72) Inventors: **GRINDERSLEV, Jakob, Bæk**; Christen Købkes Gade 19, st. th., 8000 Aarhus C (DK). **JENSEN, Torben, René**; Brombærhaven 26, 7120 Vejle Øst (DK). **YAN, Yigang**; Sichuan University Institute for New Energy and Low-carbon Technology, Chengdu, Sichuan 610017 (CN). **JØRGENSEN, Mathias**; Silkeborgvej 154, kl., 8000 Aarhus C (DK).

(74) Agent: **PLOUGMANN VINGTOFT A/S**; Strandvejen 70, 2900 Hellerup (DK).

(81) Designated States *(unless otherwise indicated, for every kind of national protection available)*: AE, AG, AL, AM, AO, AT, AU, AZ, BA, BB, BG, BH, BN, BR, BW, BY, BZ, CA, CH, CL, CN, CO, CR, CU, CZ, DE, DJ, DK, DM, DO, DZ, EC, EE, EG, ES, FI, GB, GD, GE, GH, GM, GT, HN, HR, HU, ID, IL, IN, IR, IS, JO, JP, KE, KG, KH, KN, KP, KR, KW, KZ, LA, LC, LK, LR, LS, LU, LY, MA, MD, ME, MG, MK, MN, MW, MX, MY, MZ, NA, NG, NI, NO, NZ, OM, PA, PE, PG, PH, PL, PT, QA, RO, RS, RU, RW, SA, SC, SD, SE, SG, SK, SL, SM, ST, SV, SY, TH, TJ, TM, TN, TR, TT, TZ, UA, UG, US, UZ, VC, VN, ZA, ZM, ZW.

(84) Designated States *(unless otherwise indicated, for every kind of regional protection available)*: ARIPO (BW, GH, GM, KE, LR, LS, MW, MZ, NA, RW, SD, SL, ST, SZ, TZ, UG, ZM, ZW), Eurasian (AM, AZ, BY, KG, KZ, RU, TJ, TM), European (AL, AT, BE, BG, CH, CY, CZ, DE, DK,

(54) Title: A FAST IONIC CONDUCTOR WITH STOICHIOMETRY $MG(BH_4)_2 \cdot XNH_3$

FIG. 1

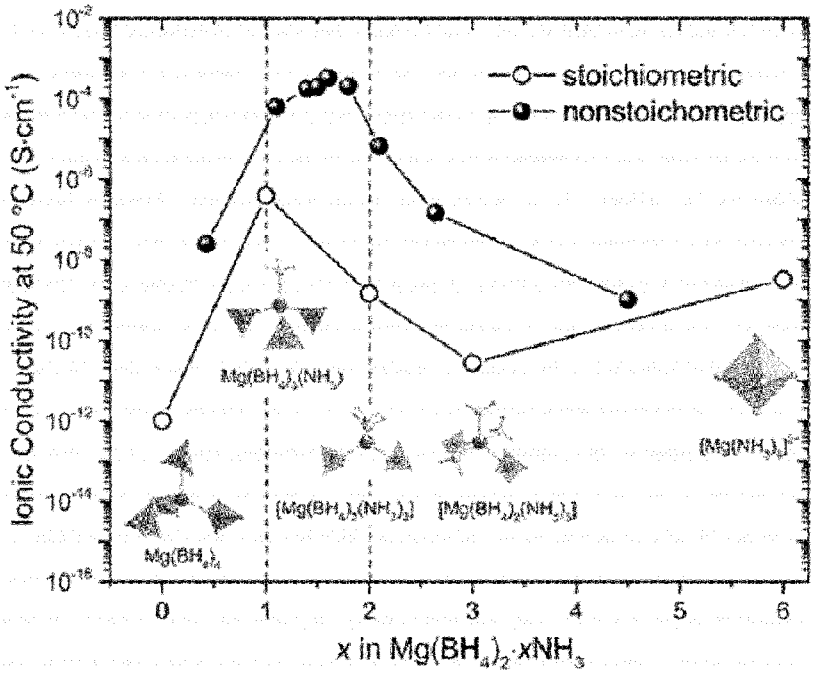

(57) Abstract: There is presented a composition of matter comprising a substance or composition with average chemical formula $Mg(BH_4)_2 \cdot xNH_3$, wherein x is non- integer $1.05<x<2.20$ and x is at least an absolute value of 0.05 away from any integer, and optionally further comprising an additive, such as an oxide optionally being in the form of nanoparticles. The composition of matter may be advantageous for being based on the abundant element magnesium and/or for exhibiting a very high ionic conductivity and/or very low electronic conductivity.

[Continued on next page]

WO 2020/053423 A1

EE, ES, FI, FR, GB, GR, HR, HU, IE, IS, IT, LT, LU, LV, MC, MK, MT, NL, NO, PL, PT, RO, RS, SE, SI, SK, SM, TR), OAPI (BF, BJ, CF, CG, CI, CM, GA, GN, GQ, GW, KM, ML, MR, NE, SN, TD, TG).

Declarations under Rule 4.17:

— *of inventorship (Rule 4.17(iv))*

Published:

— *with international search report (Art. 21(3))*

A FAST IONIC CONDUCTOR WITH STOICHIOMETRY $Mg(BH_4)_2 \cdot xNH_3$

FIELD OF THE INVENTION

The present invention relates to fast ionic conductors, such as solid electrolytes, and more particularly to a composition of matter comprising a substance or composition with average chemical formula $Mg(BH_4)_2 \cdot xNH_3$, and a corresponding method of manufacture, product by process, battery and use.

BACKGROUND OF THE INVENTION

Today, human energy consumption is mainly based on fossil fuels and we discard the spent fuel, carbon dioxide, into nature. 'Tomorrow', we need to rely on fluctuating sources of renewable energy, which occur as electricity or heat from sun and wind. Storage of this energy is essential to adapt the energy production to the oscillating human energy demand.

The success of the rechargeable lithium batteries are indisputable, but the limited progress in improving energy densities and the low abundances of Li is also becoming very clear. Therefore, alternatives are receive increasing attention.

A key challenge for development of an alternative battery is to identify a suitable solid state electrolyte. To operate a battery, a conductivity of ~1 mS cm^{-1} is often cited as the required conductivity for electrolytes with thicknesses < 25 µm. Furthermore, it may be challenging to achieve attractive ion-migration at the general operation temperature window of a rechargeable battery, *i.e.* -20 to 80 °C.

CN102659079A discloses a method for preparing a series of ammine magnesium borohydrides with different ammonia complex numbers and for use in storage of hydrogen. The procedure involves physical mixing of different ratios of $Mg(BH_4)_2$ and $Mg(BH_4)_2 \cdot 6NH_3$ in a glove box and under an atmosphere of argon. The method is challenged by the fact that the number of ammines in the produced borohydrides are integer values, e.g. $Mg(BH_4)_2 \cdot xNH_3$ for x=integer.

Hence, an improved fast ion conductor, such as a solid state electrolyte, would be advantageous, and in particular a fast ion conductor based on an abundant element, showing high ionic conductivity at the general operation temperature window of rechargeable battery would be advantageous.

SUMMARY OF THE INVENTION

In particular, it may be seen as an object of the present invention to provide a fast ion conductor that solves the above mentioned problems of the prior art with, such as being based on an abundant element, showing high ionic conductivity at the general operation temperature window of a rechargeable battery. It is a further object of the present invention to provide an alternative to the prior art.

Thus, an aspect of the present invention relates to a composition of matter comprising a substance or composition with average chemical formula $Mg(BH_4)_2 \cdot xNH_3$, wherein x is a non-integer value between 1.05 and 2.20, and x is at least an absolute value of 0.05 away from any integer.

The invention is particularly, but not exclusively, advantageous for providing a composition of matter, which may have a high ionic conductivity, such as a high ionic conductivity at 50 ºC or at 323.15 K. It may in particular be noted, that high ionic conductivity at relatively low temperatures, such as 50 ºC, may in particular be relevant for everyday applications, such as mobile electronic devices (such as laptops, smartphones) or automobiles. Another possible advantage may be that the electronic conductivity is negligible. Furthermore, a possible advantage may be that it comprises, such as consists of elements, which are abundant, such as magnesium.

Thus, another aspect of the present invention relates to a battery or an electrochemical cell comprising a composition of matter as described herein, wherein the battery or the electrochemical cell includes an electrode comprising magnesium.

Yet another aspect of the present invention relates to a method for preparing a composition of matter, wherein the method comprises the steps of:

1 - providing a mixture of α-$Mg(BH_4)_2$ and $Mg(BH_4)_2 \cdot 6NH_3$,

2 - subjecting the mixture to a mechanochemical treatment to obtain a composition of matter with average chemical formula $Mg(BH_4)_2 \cdot xNH_3$, wherein x is a non-integer value value between 1.05 and 2.20, and x is at least an absolute value of 0.05 away from any integer.

A further aspect of the present invention relates to a composition of matter prepared by a method described herein.

An additional aspect of the present invention relates to a use of a composition of matter as described herein and/or prepared according to a method described herein for conducting an ionic current.

DESCRIPTION OF THE FIGURES

Figure 1 shows ionic conductivity as a function of ammonia (NH_3) content (x) in the formula units for $Mg(BH_4)_2 \cdot xNH_3$ measured at T = 50 °C.

Figure 2 shows magnesium ionic conductivity as a function of temperature for a series of compounds $Mg(BH_4)_2 \cdot xNH_3$. (a) shows the temperature-dependent Mg^{2+}-ion conductivity of the compounds $Mg(BH_4)_2 \cdot xNH_3$, x = 1, 2, 3 and 6, compared to the composite where x=1.6. (b) Magnesium ionic conductivity as a function of temperature for highly conducting oxides and hydrides compared to the new material $1.6NH_3$@MgO.

Figure 3 shows (a) *In-situ* synchrotron radiation X-ray powder diffraction (SR PXD) of $Mg(BH_4)_2 \cdot xNH_3$ (x=1.5). (b) Differential scanning calorimetry profiles of sample x=1.5 and the composite $1.5NH_3$@MgO. (c) selected diffraction pattern of $Mg(BH_4)_2 \cdot 1.5NH_3$ before heating, compared to $Mg(BH_4)_2 \cdot 1.5NH_3$@MgO after heating and after cooling (mass ratio 1:3, donated $1.5NH_3$@MgO). Unmarked diffraction peaks are assigned to $Mg(BH_4)_2 \cdot xNH_3$, x = 1 or 2, and diffraction from MgO is marked with a circle.

Figure 4 shows a cyclic voltammogram of an Au/$1.6NH_3$@MgO/Mg cell at 60 °C.

Figures 5-16 show Rietveld refinement plots of PXD data measured at room temperature.

Figure 17 shows a Nyquist plot of the nanocomposite $Mg(BH_4)_2 \cdot 1.6NH_3/MgO$ (mass ratio 3:1), denoted $1.6NH_3@MgO$, wherein Z' is the real part and Z'' is the imaginary part of the impedance.

Figure 18 shows a cyclic voltammogram of an $Au/1.6NH_3@MgO/Au$ cell at 25 °C.

Figure 19 shows temperature dependent ionic conductivities of $Mg(BH_4)_2 \cdot xNH_3$, x=0.4, 1.1, 1.4, 1.5, 1.8, 2.1, and 4.7, and nanocomposite $1.5NH_3@MgO$.

Figure 20 shows an overview of crystal structures of $Mg(BH_4)_2 \cdot xNH_3$.

Figure 21 shows cyclic voltammograms of an $Au/1.6NH_3@MgO/Mg$ cell at 60 °C.

Figures 22-25 show *in situ* SR PXD patterns of $Mg(BH_4)_2 \cdot xNH_3$, for x=1.1, 1.4, 1.6, and 1.8.

Figure 26 shows DSC profiles of $Mg(BH_4)_2 \cdot xNH_3$ x=1, 1.5, and 2.

Figure 27 shows mass spectra of sample x=1.5 and of sample $1.5NH_3@MgO$. The results indicates that the onset decomposition temperatures is around 150 °C for sample x=1.5 and 120 °C for $1.5NH_3@MgO$.

Figure 28 shows a shape change of a pellet of $Mg(BH_4)_2 \cdot 1.5NH_3$ (a) upon heating from 30 to 70 °C, the pellet keeps the shape.

Figure 29 Figure 30 shows transmission electron microscope (TEM) images. Subfigure (a) shows MgO nanopowders (with the scalebar being 100 nm) and subfigure (b) shows $1.5NH_3@MgO$ nanocomposite (with a scalebar being 200 nm).

Figure 30 shows scanning transmission electron microscopy (STEM) image and energy-dispersive X-ray spectroscopy (EDS) of a particle of $1.5NH_3@MgO$ nanocomposite. The scale bars in the six images are 600 nm. The images shows in the upper row (from left to right): High-angle annular dark-field imaging (HAADF), Mg, O. The images shows in the lower row (from left to right): N, B, and in the last image (in the lower right corner) an overlay of O, Mg, B and N.

Figure 31 shows PXD patterns of sample $Mg(BH_4)_2 \cdot 1.6NH_3$, and the $1.6NH_3@MgO$ nanocomposite: as-synthesized and after being kept at room temperature for 40 days. The sample $Mg(BH_4)_2 \cdot 1.6NH_3$ is an as-synthesized sample (with no additive present), in which one can observe the two compounds $Mg(BH_4)_2 \cdot NH_3$ and $Mg(BH_4)_2 \cdot 2NH_3$. For $1.6NH_3@MgO$, as-synthesized and after storage for 40 dayes, one can only observe weak reflections of $Mg(BH_4)_2 \cdot 2NH_3$, because $Mg(BH_4)_2 \cdot xNH_3$, x=1 and some of x=2 are stabilized in an amorphous state owing to addition of the additive, MgO.

Figure 32 shows temperature dependent ionic conductivities of $Mg(BH_4)_2 \cdot xNH_3$, x=1.6 with, respectively, 50 wt% SiO_2 (filled circles, denoted $1.6NH_3$ + 50wt% SiO_2) and 60wt% Al_2O_3 (open squares, denoted $1.6NH_3$ + 60 wt% Al_2O_3).

Figure 33 shows a diffraction pattern for $Mg(BH_4)_2 \cdot 1.6NH_3$ at different time points. The figure shows that $Mg(BH_4)_2 \cdot 1.6NH_3$ starts to crystallize in 2 hr and fully crystallize in 24 hr after cooling down to RT.

Figure 34 shows an NMR spectra of the composite $Mg(BH_4)_2 \cdot 1.6NH_3$.

DETAILED DESCRIPTION OF THE INVENTION

Definitions

Prior to discussing the present invention in further details, the following terms and conventions will first be defined:

Non-integer

In the present context, the term ”non-integer” refers to the understanding that the x value is not an integer and optionally that the x value is at least an absolute value of 0.05 away from any integer value, such as x not being within [0;0.05[and not being within]0.95; 1.05[and not being within]1.95;2.05[.

Chemical formula

In the present context, the term “chemical formula” refers to any substance or composition having the corresponding stoichiometry. This does not necessarily imply, that a substance, such as a molecule or a crystal, with the present formula is present.

Average chemical formula

In the present context, the term “average chemical formula” refers to the understanding that the chemical formula may be representative of a substance or a composition of substances. It may thus be understood that the composition with average chemical formula $Mg(BH_4)_2 \cdot xNH_3$, is a mixture of substances with the chemical fomulas, $Mg(BH_4)_2 \cdot yNH_3$ and $Mg(BH_4)_2 \cdot zNH_3$, wherein y and z are different values representing the amount of NH_3 in each of the substances making up the composition.

Additive

In the present context, the term "additive" refers to oxides of metals or half-metals, such as, but not limited to MgO, SiO_2 and Al_2O_3. Furthermore, the additive may be a composition comprising one or more oxides. It may be understood that the composition of matter comprising the additive is a composite, such as a composite material.

Composite

In the present context, the term "composite" or 'composite material' may be understood to be a material made from two or more constituent materials with significantly different physical or chemical properties that, when combined, produce a material with characteristics different from the individual components. The individual components remain separate and distinct within the finished structure.

Eutectic system

In the present context, the term "eutectic system" refers to a homogeneous mixture of susbtances melting at a temperature lower than the melting point of either of the individual substances taken alone. A composition of matter may comprise separate regions, such as parts or areas, wherein the regions consist of an eutectic system. However, a region may also account for the whole composition. Furthermore, if the temperature of an eutectic system goes below the eutectic temperature, an amorphous solid may be formed.

Largest dimension

In the present context, the term "largest dimension" refers to the largest diameter of an irregular shape (a particle).

Mechanochemical treatment

In the present context, the term "*mechanochemical treatment*" refers to the treatment of a solid using methods that apply mechanical energy, such as, but not limited to, dry or wet ball-milling, grinding, chock pulverization etc.

Composition with average chemical formula $Mg(BH_4)_2 \cdot xNH_3$

An aspect of the present invention relates to a composition of matter comprising a substance or composition with average chemical formula $Mg(BH_4)_2 \cdot xNH_3$, wherein x is a non-integer value between 1.05 and 2.20, and x is at least an absolute value of 0.05 away from any integer.

An embodiment of the present invention relates to a composition of matter, wherein x is a non-integer value between 1.05 and 1.95.

An embodiment of the present invention relates to a composition of matter, wherein x is a non-integer value between 1.10 and 1.90.

An embodiment of the present invention relates to a composition of matter, wherein x is a non-integer value between 1.40 and 1.80.

An embodiment of the present invention relates to a composition of matter, wherein x is a non-integer value selected from the list consisting of 1.57, 1.60, and 1.78.

An embodiment of the present invention relates to a composition of matter, wherein x is 1.60.

The value of x may be confined within a certain range such as $1.05<x<1.95$, such as $1.1<x<1.9$, such as $1.2<x<1.9$, such as $1.3<x<1.9$, such as $1.4<x<1.8$, such as $1.5<x<1.7$, such as $1.55<x<1.65$, such as $1.57<x<1.63$, such as $1.575<x<1.625$. The value of x may be a certain value, such as any one of $x=1.1$, 1.4, 1.5, 1.6, or 1.8.

An advantage of the range, $1.05<x<1.95$, may be that the ionic conductivites are particularly high in this range. Another possible advantage may be that values in this range may be achieved by a mixture of substances with the chemical fomulas $Mg(BH_4)_2 \cdot NH_3$ and $Mg(BH_4)_2 \cdot 2NH_3$, respectively. Thus, the substance or composition with average chemical formula $Mg(BH_4)_2 \cdot xNH_3$ might then be formed from the binary chemical mixture of $Mg(BH_4)_2 \cdot NH_3$ and $Mg(BH_4)_2 \cdot 2NH_3$. This may be advantageous, e.g., for allowing forming a substantially eutectic system which may have a particularly high ionic conductivity. Another possible advantage may

be that it enables melting at a particularly low (and hence energy-efficient) temperature because the eutectic temperature (melting point of the mixture) is lower than the melting point of either of $Mg(BH_4)_2 \cdot NH_3$ and $Mg(BH_4)_2 \cdot 2NH_3$.

The additive

An embodiment of the present invention relates to a composition of matter, wherein the composition of matter is further comprising an additive.

An embodiment of the present invention relates to a composition of matter, wherein the additive comprises one or more oxides independently selected from the group consisting of MgO, SiO_2 and Al_2O_3.

An embodiment of the present invention relates to a composition of matter, wherein the additive is MgO.

An embodiment of the present invention relates to a composition of matter, wherein the additive comprises particles with a largest dimension being less than 1 mm.

An embodiment of the present invention relates to a composition of matter, wherein the additive comprises particles with a largest dimension being less than 10 micrometer.

An embodiment of the present invention relates to a composition of matter, wherein the additive comprises particles with a largest dimension being less than 0.1 micrometer.

An embodiment of the present invention relates to a composition of matter, wherein the additive comprises particles with a largest dimension being less than 10 nanometer.

An embodiment of the present invention relates to a composition of matter, wherein the additive is added in an amount, so that the total weight of the resulting composition of matter consist of 50 to 75 wt% additive.

An embodiment of the present invention relates to a composition of matter, wherein the additive is added in an amount, so that the total weight of the resulting composition of matter consist of 50 to 60 wt% additive.

According to an embodiment of the invention the composition of matter is further comprising an additive, such as an inert additive, such as a crystalline and inert additive. The additive may be added in an amount (with respect to the composition of matter) of at least 5 wt%, such as at least 10 wt%, such as at least 20 wt%, such as at least 25 wt%, such as at least 30 wt%, such as at least 40 wt%, such as at least 50 wt%, such as at least 60 wt%, such as at least 70 wt%, such as at least 75 wt%, such as at least 80 wt%, such as at least 90 wt%. The additive may be added in an amount (with respect to the composition of matter) of at most 90 wt%, such as at most 80 wt%, such as at most 75 wt%, such as at most 70 wt%, such as at most 60 wt%, such as at most 50 wt%, such as at most 40 wt%, such as at most 30 wt%, such as at most 25 wt%, such as at most 20 wt%, such as at most 10 wt%, such as at most 5 wt%. The additive may be added in an amount (with respect to the composition of matter) of within 20-80 wt% or within 45-80 %, such as within 25-75 wt%, such as within 30-70 wt%, such as within 40-60 wt% (reference to "within" may imply both endpoints excluded).

A possible advantage of an additive may be, that it enables stabilizing the structure of the eutectic system (which may have favourable ionic conductivity), which may be produced by decreasing the temperature from above the eutectic temperature to below the eutectic temperature. Another possible advantage may be that the additive enables increasing the ionic conductivity. The additive may, for example, comprise, such as consist of, MgO, SiO_2 or Al_2O_3. The additive may be particles dispersed in the composition of matter. Another possible advantage of comprising an additive may be that the composition of matter may be tailored to achieve certain properties, e.g., being cheaper. Another possible advantage of adding an additive, such as an additive in the form of particles, may be that it improves the mechanical properties, such makes the composition of matter harder (such as increases a Young's modulus).

The additive may be inert, which may be understood as is common in the art, and in particular as stable and unreactive towards $Mg(BH_4)_2 \cdot xNH_3$ at least under conditions of a temperature of 25 °C in an argon atmosphere with absolute pressure of 100 kPa (or 14.504 psi or 0.987 atm), less than 1 ppm CO_2, less than 1 ppm H_2O, and less than 1 ppm O_2.

According to an embodiment of the invention there is presented a composition of matter further comprising an additive, wherein the additive is an oxide, such as any one or more of, MgO, SiO_2 and Al_2O_3.. A composition of matter with an additive in the form of Al_2O_3 has also been realized. A composition of matter with an additive in the form of SiO_2 has also been realized.

According to an embodiment of the invention there is presented a composition of matter further comprising an additive, wherein the additive comprises particles with a largest dimension being less than 1 mm, such as less than 0.1 mm, such as less than 10 micrometer, such as less than 1 micrometer, such as less than 0.5 micrometer, such as less than 0.25 micrometer, such as less than 0.2 micrometer, such as less than 0.1 micrometer, such as less than 80 nm, such as less than 75 nm, such as less than 70 nm, such as less than 60 nm, such as less than 50 nm, such as less than 25 nm, such as less than 10 nanometer. Particles with a largest dimension being less than 1 mm may be referred to as microparticles. Such particles may serve to modify the properties of the composite material in which they are dispersed and/or embedded. For example, advantageous properties may be one or more of increased stability (such as capability of remaining in an amorphous phase for longer) and/or increased ionic conductivity. Another possible advantage may be that the mechanical properties is improved by the additive, for example so that a mechanically stable pellet or tablet can be prepared. An advantageous effect of modifying the properties of the composite material may be more pronounced if the largest dimension of the additive particles are even smaller, such as less than 0.1 mm, such as less than 10 micrometer, such as less than 1 micrometer, such as less than 0.5 micrometer, such as less than 0.25 micrometer, such as less than 0.2 micrometer, such as less than 0.1 micrometer, such as less than 10 nanometer.

The composition of matter, such as the composition of matter comprising an additive, may be a composite, such a microcomposite or a nanocomposite. A microcomposite and a nanocomposite may each be a multiphase solid material where one of the phases has one, two or three dimensions of less than, respectively, 100 micrometers (μm) or 100 nanometers (nm), or structures having, respectively, micro- or nano-scale repeat distances between the different phases that make up the material. Microscale may be defined as 100 nanometers-100 micrometers. Nanoscale may be defined as 100 picometers-100 nanometers.

The structure of the composition

An embodiment of the present invention relates to a composition of matter, wherein the matter comprise regions of an eutectic system.

An embodiment of the present invention relates to a composition of matter, wherein the matter comprises regions of an amorphous solid.

A beneficial effect of adding additives, such as MgO, SiO_2 and Al_2O_3 nanopowders, may that they stabilize the amorphous solid at temperatures below 55 ºC, such as at or below room temperature (where room temperature may be 25 ºC). Notice that X-ray powder diffraction down to -120 ºC was measured, and there was no crystallisation within 1 hour.

According to an embodiment of the invention there is presented a composition of matter comprising, such as consisting of one or more, regions, such as grains or crystals, having an eutectic system, such as an eutectic system for the binary chemical mixture with the two components being $Mg(BH_4)_2 \cdot NH_3$ and $Mg(BH_4)_2 \cdot 2NH_3$. A possible advantage may be that this may result in a composition of matter comprising regions having an eutectic system that may have particularly high ionic conductivity.

According to an embodiment of the invention there is presented a composition of matter comprising, such as consisting of, an amorphous or non-crystalline substance or solid. A possible advantage of this may be that a composition of matter comprising an amorphous substance or solid may have particularly high ionic conductivity.

According to an embodiment of the invention there is presented a composition of matter comprising, such as consisting of, an amorphous substance or solid, such as grains, which is capable of remaining amorphous during a period of 168 hours (or 7 days), such as 240 hours (or 10 days), such as 336 hours (or 14 days), such as 720 hours (or 30 days), such as 960 hours (or 40 days), such as 50 days. It may be understood that the capability of remaining amorphous may be at specific conditions, such as at a temperature of 298.15 K (or 25 °C) and in an argon atmosphere with absolute pressure of 100 kPa (or 14.504 psi or 0.987 atm), less than 1 ppm CO_2, less than 1 ppm H_2O, and less than 1 ppm O_2. An advantage of remaining amorphous may be that the ionic conductivity is higher in the amorphous state.

The property 'amorphous' is to be understood as is common in the art. The property 'non-crystalline' is to be understood as is common in the art. More particularly, by amorphous or non-crystalline may be understood that a degree of crystallinity, such as a degree of long-range crystalline order, is smaller than for the purely crystalline substance or composition, such as at least 5 wt%, such as at least 10 wt%, such as at least 25 wt%, such as at least 30 wt%, such as at least 50 wt%, such as at least 75 wt%, such as at least 90 wt%, such as at least 99 wt%, of the substance or composition being amorphous. The degree of crystallinity can be measured using powder X-ray diffraction (PXRD). The amount of the substance or composition may be determined with nuclear magnetic resonance (NMR) and/or the degree of crystallinity may be determined with x-ray powder diffraction (XRPD), such as using Rietveld refinement. For example, if the NMR data reveals that the composition of matter comprises $Mg(BH_4)_2{\cdot}NH_3$ and $Mg(BH_4)_2{\cdot}2NH_3$, then it is comprising an amorphous substance or solid if $Mg(BH_4)_2{\cdot}NH_3$ and/or $Mg(BH_4)_2{\cdot}2NH_3$ is amorphous, such as if at least 5 wt%, such as at least 10 wt%, such as at least 25 wt%, such as at least 30 wt%, such as at least 50 wt%, such as at least 75 wt%, such as at least 90 wt%, such as at least 99 wt%, of $Mg(BH_4)_2{\cdot}NH_3$ or of $Mg(BH_4)_2{\cdot}2NH_3$ is amorphous. In embodiments, the composition of matter comprises $Mg(BH_4)_2{\cdot}NH_3$ or $Mg(BH_4)_2{\cdot}2NH_3$ of which at least 5 wt%, such as at least 10 wt%, such as at least 25 wt%, such as at least 30 wt%, such as at least 50 wt%, such as at least 75

wt%, such as at least 90 wt%, such as at least 99 wt%, of either or both of $Mg(BH_4)_2 \cdot NH_3$ and/or $Mg(BH_4)_2 \cdot 2NH_3$ is amorphous.

Electrochemical properties

An embodiment of the present invention relates to a composition of matter, wherein the magnesium ionic conductivity at a temperature of about 50 ºC of the composition of matter is larger than $3.5x10^{-4}$ $S \cdot cm^{-1}$.

An embodiment of the present invention relates to a composition of matter, wherein the magnesium ionic conductivity at a temperature between 20 and 90 ºC of the composition of matter is equal to or larger than $1x10^{-6}$ $S \cdot cm^{-1}$.

An embodiment of the present invention relates to a composition of matter, wherein the composition of matter is compatible with metallic Mg.

An embodiment of the present invention relates to a composition of matter, wherein the electrochemical stability window is equal to or larger than 1.2 V.

An embodiment of the present invention relates to a composition of matter, wherein the electrochemical stability window is equal to or larger than 1.5 V.

An embodiment of the present invention relates to a composition of matter, wherein the electrochemical stability window is equal to or larger than 2.0 V.

An embodiment of the present invention relates to a composition of matter, wherein the electrochemical stability window is equal to or larger than 2.5 V.

According to an embodiment of the invention there is presented a composition of matter, wherein the ionic conductivity, such as the magnesium ionic conductivity "$\sigma(Mg^{2+})$", at a temperature of 50 ºC of the composition of matter is larger than $4x10^{-7}$ $S \cdot cm^{-1}$, such as equal to or larger than $5x10^{-7}$ $S \cdot cm^{-1}$ $S \cdot cm^{-1}$, such as equal to or larger than $1x10^{-6}$ $S \cdot cm^{-1}$, such as equal to or larger than $3x10^{-6}$ $S \cdot cm^{-1}$, such as equal to or larger than $1x10^{-5}$ $S \cdot cm^{-1}$, such as equal to or larger than $3x10^{-5}$ $S \cdot cm^{-1}$, such as equal to or larger than $1x10^{-4}$ $S \cdot cm^{-1}$, such as equal to or larger than $3x10^{-4}$ $S \cdot cm^{-1}$, such as equal to or larger than $3.5x10^{-4}$ $S \cdot cm^{-1}$.

A high ionic conductivity may be useful, e.g, in case the composition of matter is used as an electrolyte, a solid electrolyte and/or a fast ionic conductor in a battery. This may in particular be the case for a temperature, which is within the general operation temperature window of rechargeable battery, i.e. −20 to 80 ºC.

According to an embodiment of the invention there is presented a composition of matter, wherein the ionic conductivity, such as the magnesium ionic conductivity "$\sigma(Mg^{2+})$", at a temperature of 80 ºC of the composition of matter is larger than $6x10^{-5}$ $S{\cdot}cm^{-1}$, such as equal to or larger than $1x10^{-6}$ $S{\cdot}cm^{-1}$ $S{\cdot}cm^{-1}$, such as equal to or larger than $3x10^{-6}$ $S{\cdot}cm^{-1}$, such as equal to or larger than $1x10^{-5}$ $S{\cdot}cm^{-1}$, such as equal to or larger than $3x10^{-5}$ $S{\cdot}cm^{-1}$, such as equal to or larger than $1x10^{-4}$ $S{\cdot}cm^{-1}$, such as equal to or larger than $3x10^{-4}$ $S{\cdot}cm^{-1}$, such as equal to or larger than 1 $mS{\cdot}cm^{-1}$, such as equal to or larger than 2 $mS{\cdot}cm^{-1}$, such as equal to or larger than 2.3 $mS{\cdot}cm^{-1}$. A high ionic conductivity may be useful, e.g, in case the composition of matter is used as an electrolyte, a solid electrolyte and/or a fast ionic conductor in a battery. This may in particular be the case for a temperature, which is within the general operation temperature window of rechargeable battery, i.e. −20 to 80 ºC.

According to an embodiment of the invention there is presented a composition of matter further comprising an additive, wherein the additive has an electronic conductivity smaller than $\sigma < 10^{-7}$ S cm^{-1}, such as smaller than $\sigma<10^{-8}$ S cm^{-1}, such as smaller than $\sigma<10^{-9}$ S cm^{-1}, such as smaller than $\sigma<10^{-10}$ S cm^{-1}, such as smaller than $\sigma<10^{-11}$ S cm^{-1}, such as smaller than $\sigma<10^{-12}$ S cm^{-1}, at a temperature of 298.15 K (or 25 °C).

According to an embodiment of the invention there is presented a composition of matter, wherein the composition of matter is a fast ionic conductor, such as $\sigma(Mg^{2+})>10^{-4}$ S cm^{-1} at a temperature of 298.15 K (or 25 °C). The composition of matter may furthermore be an electrolyte, such as a solid electrolyte. A solid electrolyte has ionic conductivity (σ_i) larger than, such as at least 10^2, such as at least 10^3, such as at least 10^4, such as at least 10^5, such as at least 10^6 times larger than the electronic conductivity (σ_e).

According to an embodiment of the invention there is presented a composition of matter wherein the composition of matter is compatible with metallic magnesium. By 'compatible with metallic magnesium' may be understood that reversible magnesium (Mg) plating/stripping chemistry can be enabled. This may in particular be advantageous for enabling that metallic magnesium can be employed as electrode material in a battery where the composition of matter is employed as electrolyte, such as solid electrolyte.

According to an embodiment of the invention there is presented a composition of matter wherein the electrochemical window, such as the electrochemical stability window, (vs Mg/Mg^{2+}) is equal to or larger than 1.2 V, such as larger than 1.5 V, such as larger than 2.0 V, such as equal to or larger than 2.5 V. The electrochemical (stability) window is understood as is common in the art, such as the voltage range between which the composition or substance is neither oxidized nor reduced. The electrochemical window may be understood to be measured in an electrochemical cell at 333.15 K (or at 60 °C) vs. Mg/Mg^{2+} at a scanning rate of 10 mV/s. The measurement may start right after 20 cycles of striping/plating at a scanning rate of 10 mV/s, e.g., between −0.5 to 1.2 V.

Further aspects

Another aspect of the present invention relates to a battery or an electrochemical cell comprising a composition of matter as described herein, wherein the battery or the electrochemical cell includes an electrode comprising magnesium.

An embodiment of the present invention relates to a battery or an electrochemical cell, wherein the electrode comprises at least 98% magnesium.

Yet another aspect of the present invention relates to a method for preparing a composition of matter, wherein the method comprises the steps of:

1 - providing a mixture of α-$Mg(BH_4)_2$ and $Mg(BH_4)_2 \cdot 6NH_3$,

2 - subjecting the mixture to a mechanochemical treatment to obtain a composition of matter with average chemical formula $Mg(BH_4)_2 \cdot xNH_3$, wherein x is a non-integer value between 1.05 and 2.20, and x is at least an absolute value of 0.05 away from any integer.

A preffered embodiment of the present invention relates to a method for preparing a composition of matter, wherein the method comprises the steps of:
1 - providing a mixture of α-$Mg(BH_4)_2$ and $Mg(BH_4)_2 \cdot 6NH_3$ in a ratio comprised within the range of 1:0.175 to 1:0.325 for the two compounds respectively,
2 - subjecting the mixture to a mechanochemical treatment to obtain a composition of matter with average chemical formula $Mg(BH_4)_2 \cdot xNH_3$, wherein x is a non-integer value between 1.05 and 1.95.

An embodiment of the present invention relates to a method, for preparing a composition of matter, wherein x is a non-integer value between 1.10 and 1.90.

The mechanochemical treatment may be ball-milling. An advantage of employing mechanochemical treatment, such as ball-milling, may be that while a substance with (integer) x=2 can be made by heating x=6 in vacuum, the substance with non-integer x values can be made, such as, mechanochemically.

An embodiment of the present invention relates to a method, for preparing a composition of matter, wherein the mechanochemical treatment is ball-milling.

An embodiment of the present invention relates to a method for preparing a composition of matter, wherein an additive comprising one or more oxides independently selected from the group consisting of MgO, SiO_2, and Al_2O_3 are added subsequent to step 2, followed by annealing at a temperature between 55 and 120 °C, such as between 55 and 110, between 55 and 100, between 55 and 90, between 55 and 80, between 55 and 70, such as between 60 and 120, between 65 and 120, between 70 and 120, between 60 and 100, between 60 and 80, or between 65 and 75.

An embodiment of the present invention relates to a method for preparing a composition of matter, wherein an additive comprising one or more oxides independently selected from the group consisting of MgO, SiO_2, and Al_2O_3 are added subsequent to step 2, followed by annealing at a temperature of about 70 °C.

An embodiment of the present invention relates to a method for preparing a composition of matter, wherein MgO is added subsequent to step 2, followed by annealing at a temperature of about 70 °C.

An embodiment of the present invention relates to a method for preparing a composition of matter, wherein said method, subsequent to the mechanochemical treatment, further comprises:

a) heating the mixture above an eutectic temperature of about 55 °C,

b) cooling the mixture below the eutectic temperature.

A further aspect of the present invention relates to a composition of matter prepared by a method described herein.

An additional aspect of the present invention relates to a use of a composition of matter as described herein and/or prepared according to a method described herein for conducting an ionic current.

It should be noted that embodiments and features described in the context of one of the aspects of the present invention also apply to the other aspects of the invention.

All patent and non-patent references cited in the present application, are hereby incorporated by reference in their entirety.

The invention will now be described in further details in the following non-limiting examples.

EXAMPLES

Example 1 - synthesis procedures

The dense polymorph of magnesium borohydride, α-$Mg(BH_4)_2$ was synthesized from dimethylsulfide borane $(CH_3)_2S{\cdot}BH_3$ and dibutylmagnesium, $Mg(n Bu)_2$. $(CH_3)_2S{\cdot}BH_3$ (10 mL, 10 M), $Mg(n Bu)_2$ (28 mL, 1 M) and toluene (40 mL) were mixed in a 250 mL filterflask, sealed in argon atmosphere. The mixture was left to

stir for 1 day, after which the filtrate was removed by filtration. The white precipate was dried under dynamic vacuum for 1 hour at room temperature, after which it was transferred to three separate Schlenk tubes, heated to 140 °C for 2 hours in argon atmosphere, followed by 2 hours under dynamic vacuum. All sample handling are carried out using standard Schlenk techniques and argon glovebox.

$Mg(BH_4)_2 \cdot 6NH_3$ was synthesized by exposure of α-$Mg(BH_4)_2$ to dry ammonia gas at a pressure of 1 bar for 2 h at room temperature. $Mg(BH_4)_2 \cdot 3NH_3$ and $Mg(BH_4)_2 \cdot 2NH_3$ were obtained by heating $Mg(BH_4)_2 \cdot 6NH_3$ at 63 °C for 6 h and 90 °C for 4 h in dynamic vacuum, respectively. Composites $Mg(BH_4)_2 \cdot xNH_3$ (x=0.4, 0.9, 1.1, 1.4, 1.5, 1.6, 1.8, 2.1, 2.6, 4.5) and substance $Mg(BH_4)_2 \cdot xNH_3$ (x=1.0) were synthesized by ball-milling of $Mg(BH_4)_2 \cdot 6NH_3$ and α-$Mg(BH_4)_2$ in individual molar ratios for 2 hours. The ball-milling was carried out for 2 min with a 2 min pause for 60 repetitions at a speed of 200 rpm and a ball-to-powder weight ratio of 30:1. The powders were loaded under inert argon atmosphere in a 80 mL tungsten carbide coated steel vial.

An additive may be added, such as MgO (e.g., 75 wt%), SiO_2 (e.g., 50 wt %) or Al_2O_3 (e.g., 60 wt%). $Mg(BH_4)_2 \cdot 1.6NH_3$ with additive MgO, denoted, $1.6NH_3$@MgO, was synthesized by ball-milling the as-synthesized $Mg(BH_4)_2 \cdot 1.6NH_3$ and MgO in a mass ratio of 1 to 3 for 1 h. The powder was then annealed at 70 °C for 1 hour. Similar route was applied for the additives SiO_2 and Al_2O_3, albeit with mass ratio of $Mg(BH_4)_2 \cdot 1.6NH_3$ to oxide exchanged, respectively, to 1:1 ($Mg(BH_4)_2 \cdot 1.6NH_3$:SiO_2) and 1:1.5 ($Mg(BH_4)_2 \cdot 1.6NH_3$:Al_2O_3).

Example 2 - characterization

Instruments and methods

Powder X-ray Diffraction (PXD) data were collected at room temperature (RT) on a Rigaku SMARTLAB diffractometer, equipped with a rotating Cu anode (Cu Kα radiation, 2 kW, λ = 1.54053 Å). The samples were packed in 0.5 mm o.d. capillary tubes in the glovebox, sealed with glue, and transferred to the instrument without air exposure.

In situ synchrotron radiation powder X-ray diffraction (SR-PXD) data of the $Mg(BH_4)_2 \cdot xNH_3$ were collected from X04SA beamline at Paul Scherrer Institute (PSI), Switzerland with λ = 0.708481 Å.

The crystal structure of $Mg(BH_4)_2 \cdot NH_3$ was solved from the measured SR-PXD pattern using the program FOX.

Electrochemical Impedance Spectroscopy data were collected on a BioLogic MTZ-35 impedance analyser equipped with a high temperature sample holder. Samples were pressed into 6.35 mm diameter pellets of ca. 1 mm thickness under the pressure of 0.63 GPa. All measurements were conducted in an argon atmosphere and the temperature was measured by a K-type thermocouple 5 mm from the sample. Impedance data were measured at 20 mV ac from 3 MHz to 1 Hz. Ion conductivity data were derived from Nyquist impedance plots using the x-intercept of the Nyquist semicircle (R), area of the pellet face (A) and pellet thickness (t) according to: $\sigma = t/(R \times A)$.

Thermogravimetric analysis (TGA) and Differential scanning calorimetry (DSC) was conducted on a PerkinElmer STA 6,000, where 3–5 mg samples were placed in Al crucibles and heated at 5 °C per min under constant argon flow (50 $mL \cdot min^{-1}$).

Tunneling electron microscope (TEM) images were recorded on a FEI Talos F200X scanning/transmission electron microscope.

Results

Hexaamine magnesium borohydride, $Mg(BH_4)_2 \cdot 6NH_3$ was prepared *via* a solid-gas reaction of $Mg(BH_4)_2$ with NH_3 under ambient conditions. Compounds with integer values of, x = 2 and 3 were synthesized by heating of $Mg(BH_4)_2 \cdot 6NH_3$ in vacuum. Compounds with an integer value of x = 1 and composites with non-integer values, $0<x<6$, of $Mg(BH_4)_2 \cdot xNH_3$, were synthesized by mechanochemical treatment of appropriate amounts of $Mg(BH_4)_2 \cdot 6NH_3$ and $Mg(BH_4)_2$. Composites are formed comprising, such as consisting of, two compounds with integer x-value just above or below the average ammonia content. These materials are characterized by powder X-ray diffraction as shown in Figures 5-16. The ionic conductivities were calculated from the Nyquist plots and electrochemical data is

provided in Figure 17. Notice, that Nyquist plots consisting of a single semicircle and an electrode polarization spike is characteristic of pure ionic conductivity.

Figures 5-8 show Rietveld refinement plots of PXD data measured at room temperature, λ = 1.54056 Å, for $Mg(BH_4)_2 \cdot xNH_3$ (x = 1, 2, 3, 6), showing experimental (circles) and calculated (lines) PXD patterns, and a difference plot below (black line, shown in the bottom of each figure). Final discrepancy factors, R_p and R_{wp} (not corrected for background), and global χ^2 are shown. Table 1 provide structural data for $Mg(BH_4)_2 \cdot NH_3$ extracted from the Rietveld refinement.

Figures 9-11 show Rietveld refinement plots of PXD data measured at room temperature, λ = 0.70848 Å, for $Mg(BH_4)_2 \cdot xNH_3$ (x = 0.4, 0.9, 2.1), showing experimental (circles) and calculated (lines) PXD patterns, and a difference plot below (black line, shown in the bottom of each figure). Final discrepancy factors, R_p and R_{wp} (not corrected for background), and global χ^2 are shown.

Figures 12-16 show Rietveld refinement plots of PXD data measured at room temperature, λ = 0.70848 Å, for $Mg(BH_4)_2 \cdot xNH_3$ (x = 1.1, 1.4, 1.5, 1.6, 1.8), showing experimental (circles) and calculated (lines) PXD patterns, and a difference plot below (black line, shown in the bottom of each figure). Final discrepancy factors, R_p and R_{wp} (not corrected for background), and global χ^2 are shown.

Figure 17 shows a Nyquist plot of the nanocomposite $Mg(BH_4)_2 \cdot 1.6NH_3 \cdot MgO$ (mass ratio 3:1), denoted $1.6NH_3$@MgO, wherein Z' is the real part and Z'' is the imaginary part of the impedance. A single semicircle and an electrode polarization spike are observed. Also, the curve shape is characteristic for mass transfer of ionic charge carriers in the solid state.

Figure 1 shows ionic conductivity as a function of ammonia (NH_3) content (x) in the formula units for $Mg(BH_4)_2 \cdot xNH_3$ measured at T = 50 °C – all crystalline compounds. Samples were pressed into 6.35 mm diameter pellets of ca. 1 mm thickness under the pressure of 0.63 GPa. To improve the contact, the powders were pressured in between two Au foils (thickness of 0.1 mm) forming a Au/sample/Au symmetric cell. The cell was heated to 50 °C with a ramp of 1

°C/min and kept for 60 min before the impedance measurement was started. Impedance data were recorded at 20 mV ac from 3 MHz to 1 Hz.

The "stoichiometric" compounds, $Mg(BH_4)_2 \cdot xNH_3$ with x having integer values (x having values of 0, 1, 2, 3 and 6, see Table 2) are shown as open spheres whereas "non-stoichiometric" composites with x having non-integer values (x having values of 0.4, 1.1, 1.4, 1.5, 1.6, 1.8, 2.1, 2.6 and 4.7) are black circles. By "stoichiometric" and "non-stoichiometric" is understood, respectively, integer and non-integer x-values, and non-stoichiometric does not imply that the material is homogeneous. The structural drawings illustrate the coordination of magnesium for the stoichiometric composition. Magnesium is shown as the largest spheres, boron as smaller spheres, nitrogen still smaller spheres and hydrogen is shown as the smallest spheres.

The Mg^{2+} ionic conductivities measured at T = 50 °C are illustrated in Figure 1 as a function of NH_3 molecules in the compounds and composites, $Mg(BH_4)_2 \cdot xNH_3$. None of the substances or compositions have been heated above 50 °C. The highest Mg^{2+}-ion conductivity of the compounds (i.e., with x being an integer) is observed of $Mg(BH_4)_2 \cdot NH_3$, $\sigma(Mg^{2+}) = 4.0 \times 10^{-7}$ S cm^{-1} (at T = 50 °C), whereas the other show lower conductivities of 1.5×10^{-9}, 2.7×10^{-11} and 3.3×10^{-9} S cm^{-1}, of $Mg(BH_4)_2 \cdot 2NH_3$, $Mg(BH_4)_2 \cdot 3NH_3$ and $Mg(BH_4)_2 \cdot 6NH_3$, respectively. The composites with non-integer average x-values clearly has higher Mg^{2+} conductivities in particular those in the eutectic system comprising $Mg(BH_4)_2 \cdot NH_3$ and $Mg(BH_4)_2 \cdot 2NH_3$, with the maximum value $\sigma(Mg^{2+}) = 3.5 \times 10^{-4}$ S cm^{-1} measured for x = 1.6, *i.e.* system comprising $0.4Mg(BH_4)_2 \cdot NH_3$ and $0.6Mg(BH_4)_2 \cdot 2NH_3$, denoted $Mg(BH_4)_2 \cdot 1.6NH_3$. We note, that this value is more than 8 orders of magnitudes higher than that of the precursor, $Mg(BH_4)_2$, $\sigma(Mg^{2+}) \sim 1.0 \times 10^{-12}$ S cm^{-1}.

Figure 2 shows magnesium ionic conductivity as a function of temperature for the series of compounds $Mg(BH_4)_2 \cdot xNH_3$, x = 1, 2, 3 and 6, the composites x=1.6 (a), and the nanocomposite $Mg(BH_4)_2 \cdot 1.6NH_3$/MgO (1:3 w/w), denoted $1.6NH_3$@MgO. (b) Magnesium ionic conductivity as a function of temperature for highly conducting oxides and hydrides compared to the new material $1.6NH_3$@MgO.

Figure 2a shows the temperature-dependent Mg^{2+}-ion conductivity of the compounds $Mg(BH_4)_2 \cdot xNH_3$, x = 1, 2, 3 and 6, compared to the composite where x=1.6. Conductivity of other selected compositions are shown in Figure 19. The stoichiometric compounds, *x* = 1, 2, 3 and 6, reveal a linear increase of Mg^{2+} conductivity. The slope of the conductivity data for the composite x = 1.6 reveal an impressive decrease of activation energy for the Mg-ion conductivity by a factor ten from E_a = 3.0 eV (at T < 55 °C) to 0.3 eV (at T > 55 °C), with an impressive conductivity of $\sigma(Mg^{2+})$ = 2.0 mS cm^{-1} at 55 °C. This highly conductive state can be stabilized with MgO nanoparticles to obtain high Mg-ion conductivity at low temperature, such as below 55 ºC (or 328.15 K), such as 22-55 ºC (or 295.15-328.15 K). The nanocomposite $Mg(BH_4)_2 \cdot 1.6NH_3$/MgO (mass ratio 3:1), denoted $1.6NH_3$@MgO, has conductivities of $2.2\times10^{-6} < \sigma(Mg^{2+}) < 3.6\times10^{-3}$ S cm^{-1} in the temperature range 20 to 90 °C, and with an apparent activation energy E_a = 1.0 eV. It is noted that the composition of matter, such as the nanocomposite $Mg(BH_4)_2 \cdot 1.6NH_3$/MgO (mass ratio 3:1), denoted $1.6NH_3$@MgO, may be useful and applicable in a broad temperature range, such as in the temperature region [-20; +90] ºC, such as in the temperature region [+20; +90] ºC,

Another nanocomposite, $1.5NH_3$@MgO, has similar conductivities of $3.6\times10^{-6} < \sigma(Mg^{2+}) < 8.5\times10^{-4}$ S cm^{-1} in the temperature range 26 to 80 °C and activation energy of E_a = 0.93 eV (Figure 19). Interestingly, the conductivity of composite x=1.6, *e.g.* 3.5×10^{-4} S cm^{-1} at 50 °C, is even higher than that of x=1.5, *e.g.* 2×10^{-4} S cm^{-1} at 50 °C, and the latter possesses the eutectic system (in the eutectic system formed from the binary chemical mixture of $Mg(BH_4)_2 \cdot NH_3$ and $Mg(BH_4)_2 \cdot 2NH_3$. In parallel, the nanocomposite $1.6NH_3$@MgO (PXD pattern in Figure 21) is also more conductive than $1.5NH_3$@MgO, *i.e.* $\sigma(Mg^{2+}) = 2.3\times10^{-3}$ and 8.5×10^{-4} S cm^{-1} at 80 °C, respectively.

Figure 32 shows temperature dependent ionic conductivities of $Mg(BH_4)_2 \cdot 1.6NH_3$, respectively, 50wt% SiO_2 (filled circles, denoted $1.6NH_3$ + 50wt% SiO_2) and 60wt% Al_2O_3 (open squares, denoted $1.6NH_3$ + 60wt% Al_2O_3).

Figure 21 shows cyclic voltammograms of an Au/$1.6NH_3$@MgO/Mg cell at 60 °C. Scanning rate: 10 mV/s. This measurement started right after 20 cycles of striping/plating at a scanning rate of 10 mV/s between -0.5 to 1.2 V.

The conductivity of the $1.6NH_3$@MgO composite is compared to other inorganic Mg-ion conductors in Figure 2b. Metal oxides reaches conductivities in the order of ~1 mS cm^{-1}, but only at high temperatures, T > 600 °C. The chalgogenide, $MgSc_2Se_4$, has in fact very low ionic conductivity of $\sigma(Mg^{2+}) < 10^{-8}$ S cm^{-1} (at room temperature) and similar electronic conductivity of $\sigma_e = 10^{-10}$ S cm^{-1} at room temperature. Complex metal hydrides, such as $Mg(BH_4)(NH_2)$ and Mg(ethylenediamine)$(BH_4)_2$, exhibit a conductivity of ~10^{-6} S cm^{-1} at T = 150 °C and 6×10^{-5} S cm^{-1} at T = 70 °C, respectively. Thus, the $1.6NH_3$@MgO composite shows the highest Mg-ion conductivity at near room temperature, *i.e.* $\sigma(Mg^{2+})$ = $2.3x10^{-3}$ S cm^{-1} at 80 °C, which matches the general operation temperature window of a rechargeable battery, *i.e.* −20 to 80 °C.

The electronic conductivity is measured to $\sigma_e = 3.9\times10^{-9}$ S cm^{-1} at 25 °C by linear fitting between 0 and 1.0 V of a symmetric Au/$1.6NH_3$@MgO/Au cell (Figure 18).

Figure 18 shows a cyclic voltammogram of an Au/$1.6NH_3$@MgO/Au cell at 25 °C. The size of the $1.6NH_3$@MgO pellet: 0.5 mm in thickness, 6.4 mm in diameter. Linear fitting between 0 and 1.0 V of a symmetric Au/$1.6NH_3$@MgO/Au cell generates a resistance of 4.2×10^7 Ω, corresponding to the conductivity of 3.9×10^{-9} S cm^{-1}. The electronic conductivity of $Mg(BH_4)_2\cdot1.6NH_3$ is $\sigma_e = 7\times10^{-9}$ S cm^{-1} at 25 °C.

The composites, $Mg(BH_4)_2\cdot xNH_3$, x non-integer, all comprises, such as consists of, two compounds with integer x values. This is clearly demonstrated by ^{25}Mg solid state magic angle spinning (MAS) NMR, which reveal a single sharp resonance from the individual compounds $Mg(BH_4)_2\cdot NH_3$ and $Mg(BH_4)_2\cdot 2NH_3$. Two resonances, identical to those observed of $Mg(BH_4)_2\cdot NH_3$ and $Mg(BH_4)_2\cdot 2NH_3$, are measured for the composite $Mg(BH_4)_2\cdot 1.5NH_3$. This observation further documents that $Mg(BH_4)_2\cdot 1.5NH_3$ is a physical mixture prepared mechano-chemically from $Mg(BH_4)_2\cdot NH_3$ and $Mg(BH_4)_2\cdot 2NH_3$.

In situ synchrotron radiation powder X-ray diffraction (SR XRPD) is measured of the composite, $Mg(BH_4)_2\cdot 1.5NH_3$ upon heating from 22 to 70 °C and further upon cooling from 70 to −120 °C (Figures 22-25). Bragg reflections of both $Mg(BH_4)_2\cdot NH_3$ and $Mg(BH_4)_2\cdot 2NH_3$ disappear simultaneously at 55 °C leaving a broad hump in the diffraction background in the remaining experiment. This is a

significantly lower melting temperature as compared to the individual components, $T_{mp}(Mg(BH_4)_2 \cdot NH_3)$ = 90 °C and $T_{mp}(Mg(BH_4)_2 \cdot 2NH_3)$ = 110 °C. Further *in situ* diffraction experiments of composites with x < 1.5 reveal diffraction of $Mg(BH_4)_2 \cdot NH_3$ after initial melting at 55 °C (Figures 22-23) and of $Mg(BH_4)_2 \cdot 2NH_3$ for x > 1.5 after initial melting at 55 °C (Figures 24-25).

Figure 26 shows DSC profiles of $Mg(BH_4)_2 \cdot xNH_3$, x=1, 1.5, 2 (where x=1.5 corresponds to the lowest curve having the lowest max-temperature point of the three curves, x=1 corresponds to the middle curve with the max-temperature point being in the middle of the three curves, and x=2 being the uppermost curve with the highest max-temperature point).

Thermal analysis (DSC) of $Mg(BH_4)_2 \cdot 1.5NH_3$ displays an endothermic event at 55 °C, assigned to eutectic melting of the composite. However, no DSC signal upon cooling to −70 °C is observed, which reveal that the molten phase can readily be under-cooled and only slowly and after some time (>10 min) start to crystallise (Figure 3b, see also Figure 33 for XRPD of $Mg(BH_4)_2 \cdot 1.6NH_3$ at different timepoints). Simultaneous measurement of mass spectrometry reveal no gas release (*e.g.* H_2, NH_3 or B_2H_6), at T < 120 °C (Figure 27). This shows that the composite does not decompose and is stable also in the molten state. Photographic inspection of a pellet of $Mg(BH_4)_2 \cdot 1.5NH_3$ reveals that the shape is preserved also at 60 °C but with the material becoming softer (Figure 28). Thus, we conclude that the composition comprising $Mg(BH_4)_2 \cdot NH_3$ and $Mg(BH_4)_2 \cdot 2NH_3$ is a eutectic melt, with eutectic temperature T_{mp} = 55 °C, where a liquid phase with high viscosity is formed. If the temperature goes below the eutectic temperature, an amorphous substance or solid is formed (which amorphous substance or solid might not be stable at room temperature, at least on a timescale of one or more weeks). If the resulting composition or substance is kept at room temperature, it slowly starts to crystallize and after a few hours or days (such as 7, 10, 14, 30 or 40 hours, or such as 7, 10, 14, 30 or 40 days) it crystallizes into the two crystalline components, $Mg(BH_4)_2 \cdot NH_3$ and $Mg(BH_4)_2 \cdot 2NH_3$. The composite with additive (e.g. MgO or Al_2O_3) forms a 'stable' amorphous, or under-cooled liquid phase for at least 1.5 months. The composite, x=1.5 without additive will crystallise ca. 2 h after it has been melted at T > 55 °C, and again cooled to T < 55 °C (see data showing that $Mg(BH_4)_2 \cdot xNH_3$, x=1.6 starts to crystallize in 2 hr and fully crystallize in 24 hr in Figure 33).

Figure 27 shows a mass spectra of sample x=1.5 and of sample 1.5NH_3@MgO (Ar flow: 40 ml/min, 5 °C/min). The results indicate that the onset decomposition temperatures are around 150 °C for a sample x=1.5 and 120 °C for 1.5NH_3@MgO.

Figure 3 shows (a) *In-situ* synchrotron radiation X-ray powder diffraction (SR PXD) of $Mg(BH_4)_2 \cdot xNH_3$ (x=1.5), slow heating 22 to 70 °C followed by faster cooling to −120 °C (λ = 0.70848 Å). (b) Differential scanning calorimetry profiles of sample x=1.5 and the composite 1.5NH_3@MgO. (c) selected diffraction pattern of $Mg(BH_4)_2 \cdot xNH_3$ (x=1.5) before heating, compared to $Mg(BH_4)_2 \cdot 1.5NH_3$–MgO after heating and after cooling (mass ratio 1:3, donated 1.5NH_3@MgO). Unmarked diffraction peaks are assigned to $Mg(BH_4)_2 \cdot xNH_3$, x = 1 or 2, and diffraction from MgO is marked with a circle (λ = 0.70848 Å).

Nano structuring by mechanochemical treatment of $Mg(BH_4)_2 \cdot 1.5NH_3$/MgO (1:3 w/w), followed by annealing at 70 °C for 1 h (denoted 1.5NH_3@MgO) is utilized to stabilize the phase formed upon heating above 55 °C. Transmission electron microscopy (TEM) images reveal typical particle sizes of equal to or less than 50 nm (figure 29) and scanning transmission electron microscope (STEM) images confirm an even distribution of B and N originating from the composite $Mg(BH_4)_2 \cdot 1.5NH_3$ in 1.5NH_3@MgO (Figure 30). Thermal analysis (DSC) reveals no obvious thermal events in the temperature range from −70 to 80 °C (Figure 3b), which indicates a high level of stability (in contrast with the lack of stability – in comparison – for $Mg(BH_4)_2 \cdot 1.5NH_3$). Powder X-ray diffraction of 1.5NH_3@MgO, as synthesised and after storing 10 or 30 days at RT, only shows diffraction from MgO. Furthermore, photographic inspection reveals that the pellet of 1.5NH_3@MgO remains hard with no sign of deformation after heat treatment at 80 °C (as observed by measuring the pellet with an electronic Vernier caliper before and after heating at 80 °C and in each case obtaining a diameter of 6.43 mm).

Figure 31 shows PXD patterns of sample $Mg(BH_4)_2 \cdot 1.6NH_3$, and the 1.6NH_3@MgO nanocomposite: as-synthesised and after being kept at room temperature for 40 days. Cu Kα, λ=1.54056 Å. The sample $Mg(BH_4)_2 \cdot 1.6NH_3$ is the as-synthesised sample, in which one can clearly see two compounds, that is $Mg(BH_4)_2 \cdot xNH_3$, x=1 and x=2. In the 1.6NH_3@MgO, one can only observe weak reflections from

$Mg(BH_4)_2 \cdot xNH_3$, x=2. That is because $Mg(BH_4)_2 \cdot xNH_3$, x=1 and some of x=2 are stabilised in an amorphous state, such as molten phase, owing to addition of MgO.

To repeat, if there is no additive, such as MgO, x=1.6 sample will recrystallise completely in 24 h.

Figure 33 shows a diffraction pattern for $Mg(BH_4)_2 \cdot 1.6NH_3$ at different time points. More particularly, the figure shows diffraction patterns for $Mg(BH_4)_2 \cdot 1.6NH_3$ for an as-synthesised sample (where diffraction peaks are observed for each of $Mg(BH_4)_2 \cdot xNH_3$, x=1 and x=2), and then after cooling down to RT, more specifically at time points 10 minutes, 1 hour, 2 hours and 24 hours after cooling down to RT. The figure shows that $Mg(BH_4)_2 \cdot xNH_3$, x=1.6 starts to crystallise in 2 hr and fully crystallise in 24 hr in after cooling down to RT.

Figure 4 shows a cyclic voltammogram of an Au/$1.6NH_3$@MgO/Mg cell at 60 °C. The inset shows the Mg stripping current as a function of cycle number. The curves are shown for cycles 1, 2, 5 and 10 with Mg plating in the left-hand side (i.e., for voltages below -0.1 V) and striping in the right hand side (i.e., for voltages above -0.1 V). For the left hand side with plating, the curves (at least the low-voltage end-points) are displaced vertically (along the current density axis) to each other with the curve for 10 cycles being at the bottom, the curve for 5 cycles being above that, the curve for 2 cycles being above that and the curve for 1 cycle being topmost. For the right hand side with stripping, the curves (at least the top-points) are displaced vertically (along the current density axis) to each other with the curve for 1 cycle being at the bottom, the curve for 2 cycles being above that, the curve for 5 cycles being above that and the curve for 10 cycles being topmost.

The $1.6NH_3$@MgO nanocomposite is selected for cyclic voltammetry measurement to confirm the direct Mg-ion conduction through the electrolyte. An asymmetric Au/$1.6NH_3$@MgO/Mg cell was assembled and tested at 60 °C. As shown in Figure 4, the onset of cathodic current attributed to the Mg plating on the Au working electrode is observed at −0.1 V. The anodic current during the reverse sweep between −0.1 and 0.5 V is owing to Mg stripping. The currents of plating/stripping increase during the first ten cycles (see Figure 4 inset), implying that the interfacial contact between electrodes and electrolyte is improved during the initial cycling. No significant currents due to electrolyte decomposition is detected in the

scanned voltage range. The electrochemical stability window of 1.2 V is compatible with typical cathode materials for Mg-ion batteries such as $TiSe_2$ (1.0 V *vs* Mg/Mg^{2+}), Mo_6S_8 (1.1 V *vs* Mg/Mg^{2+}), and Ti_2S_4 (1.2 V *vs* Mg/Mg^{2+}). In the following striping/plating cycles between −0.5 and 2.5 V, irreversible oxidation > 1.2 V is observed (Supplementary Figure 21). However, the interface layer formed owing to the irreversible oxidation is able to conduct Mg ions and further improve the electrochemical stability. At 40th cycle, no obvious oxidation is observed below 2.5 V and stable striping/plating is observed up to 60 cycles indicating the high stability of the interface layer. This finding will benefit the application of the $1.6NH_3$@MgO composite as a solid electrolyte for Mg-ion battery, *i.e.* the over-potential charging will not damage the electrolyte.

Figure 34 shows an NMR spectra of the composite $Mg(BH_4)_2 \cdot 1.6NH_3$. The two compounds $Mg(BH_4)_2 \cdot NH_3$ and $Mg(BH_4)_2 \cdot 2NH_3$ have distinct ^{11}B MAS NMR resonances. $Mg(BH_4)_2 \cdot NH_3$ have two resonances with peak values at –40.4 ppm and –40.8 ppm. $Mg(BH_4)_2 \cdot 2NH_3$ have two resonances with peak values at –41.6 ppm and –42.2 ppm. The ^{11}B MAS NMR data measured of the composite, $Mg(BH_4)_2 \cdot 1.6NH_3$, i.e. $0.4Mg(BH_4)_2 \cdot NH_3$–$0.6Mg(BH_4)_2 \cdot NH_3$, 10 min after melting the sample (heated to 70 °C for 15 min) show one sharp resonance at –40.4 ppm and two weak signals at –41.6 ppm and –42.2 ppm, the latter assigned to $Mg(BH_4)_2 \cdot 2NH_3$. The sharp intense signal account for about 70 % of boron in the sample. This signal has only very weak spinning side bands in contrast to the resonances from $Mg(BH_4)_2 \cdot 2NH_3$, which have many. The sharp resonance at –40.4 ppm is assigned to high symmetry and/or dynamics (e.g. similar to liquid state) of boron in this part of the sample, i.e. the under-cooled eutectic melt. The ^{11}B MAS NMR spectrum after 1300 min is mainly a sum of spectra of $Mg(BH_4)_2 \cdot NH_3$ and $Mg(BH_4)_2 \cdot 2NH_3$ with a small contribution from the molten state of the sample.

Table 1. Structure data of $Mg(BH_4)_2 \cdot NH_3$ extracted from Rietveld refinement.

Atom	**x / a**	**y / b**	**z / c**	**Wyckoff site**	**Occupancy**
B1	0.50000	0.50000	0.50000	4a	1
H11	0.56403	0.41279	0.39145	8d	0.5
H12	0.53049	0.65397	0.49965	8d	0.5
H13	0.50477	0.44475	0.66684	8d	0.5
H14	0.40029	0.48929	0.44337	8d	0.5
B2	0.1908(3)	0.75000	0.5201(4)	4c	1
H21	0.0907(3)	0.75000	0.5792(4)	4c	1
H22	0.2594(3)	0.75000	0.6609(4)	4c	1
H23	0.2078(3)	0.87959	0.4201(4)	8d	1
N	0.6283(3)	0.25000	0.8916(4)	4c	1
H31	0.5937(3)	0.36051	0.9422(4)	8d	1
H32	0.7089(3)	0.25000	0.9486(4)	4c	1
Mg	0.6210(2)	0.25000	0.5939(2)	4c	1

Table 2. Summary of structural information for $Mg(BH_4)_2 \cdot xNH_3$.

x	**Crystal system**	***Space group***	**Lattice parameter / Å**
0	Cubic (γ-phase)	*Ia-3d*	15.7575(16)
1	Orthorhombic	*Pnma*	11.2938(1), 7.6224(1), 6.8182(1)
2	Orthorhombic	*Pcab*	17.4872(4), 9.4132(2), 8.7304(2)
3	Orthorhombic	*Pnma*	11.4328, 8.0869, 9.4379
6	Cubic	*Fm-3m*	10.7879

CLAIMS

1. A composition of matter comprising a substance or composition with average chemical formula $Mg(BH_4)_2 \cdot xNH_3$, wherein x is a non-integer value between 1.05 and 2.20, and x is at least an absolute value of 0.05 away from any integer.

2. The composition of matter according to any one of the preceding claims, wherein x is a non-integer value between 1.05 and 1.95.

3. The composition of matter according to any one of the preceding claims, wherein the composition of matter is further comprising an additive.

4. The composition of matter according to claim 3, wherein the additive comprises one or more oxides independently selected from the group consisting of MgO, SiO_2 and Al_2O_3.

5. The composition of matter according to any one of claims 3 to 4, wherein the additive comprises particles with a largest dimension being less than 1 mm.

6. The composition of matter according to any one of the preceding claims, wherein the matter comprises regions of an eutectic system.

7. The composition of matter according to any one of the preceding claims, wherein the matter comprises regions of an amorphous substance.

8. The composition of matter according to any one of the preceding claims, wherein the magnesium ionic conductivity at a temperature between 20 and 90 ºC of the composition of matter is equal to or larger than $1x10^{-6}$ $S \cdot cm^{-1}$.

9. The composition of matter according to any one of the preceding claims, wherein the composition of matter is compatible with metallic Mg.

10. The composition of matter according to any one of the preceding claims, wherein the electrochemical stability window is equal to or larger than 1.2 V.

11. A battery or an electrochemical cell comprising a composition of matter according to any one of the preceding claims, wherein the battery or the electrochemical cell includes an electrode comprising magnesium.

12. A method for preparing a composition of matter, wherein the method comprises the steps of:

1 - providing a mixture of α-$Mg(BH_4)_2$ and $Mg(BH_4)_2 \cdot 6NH_3$,

2 - subjecting the mixture to a mechanochemical treatment to obtain a composition of matter with average chemical formula $Mg(BH_4)_2 \cdot xNH_3$, wherein x is a non-integer value between 1.05 and 2.20, and x is at least an absolute value of 0.05 away from any integer.

13. The method according to claim 12, wherein an additive comprising one or more oxides independently selected from the group consisting of MgO, SiO_2, and Al_2O_3 are added subsequent to step 2, followed by annealing at a temperature between 55 and 120 °C.

14. The method according to any one of claims 12 and 13, wherein said method, subsequent to the mechanochemical treatment, further comprises:

a) heating the mixture above an eutectic temperature of about 55 °C,

b) cooling the mixture below the eutectic temperature.

15. A composition of matter prepared according to any one of claims 12 to 14.

16. Use of a composition of matter according to claim 15 or anyone of claims 1 to 10 and/or prepared according to a method of any one of claims 12 to 14, for conducting an ionic current.

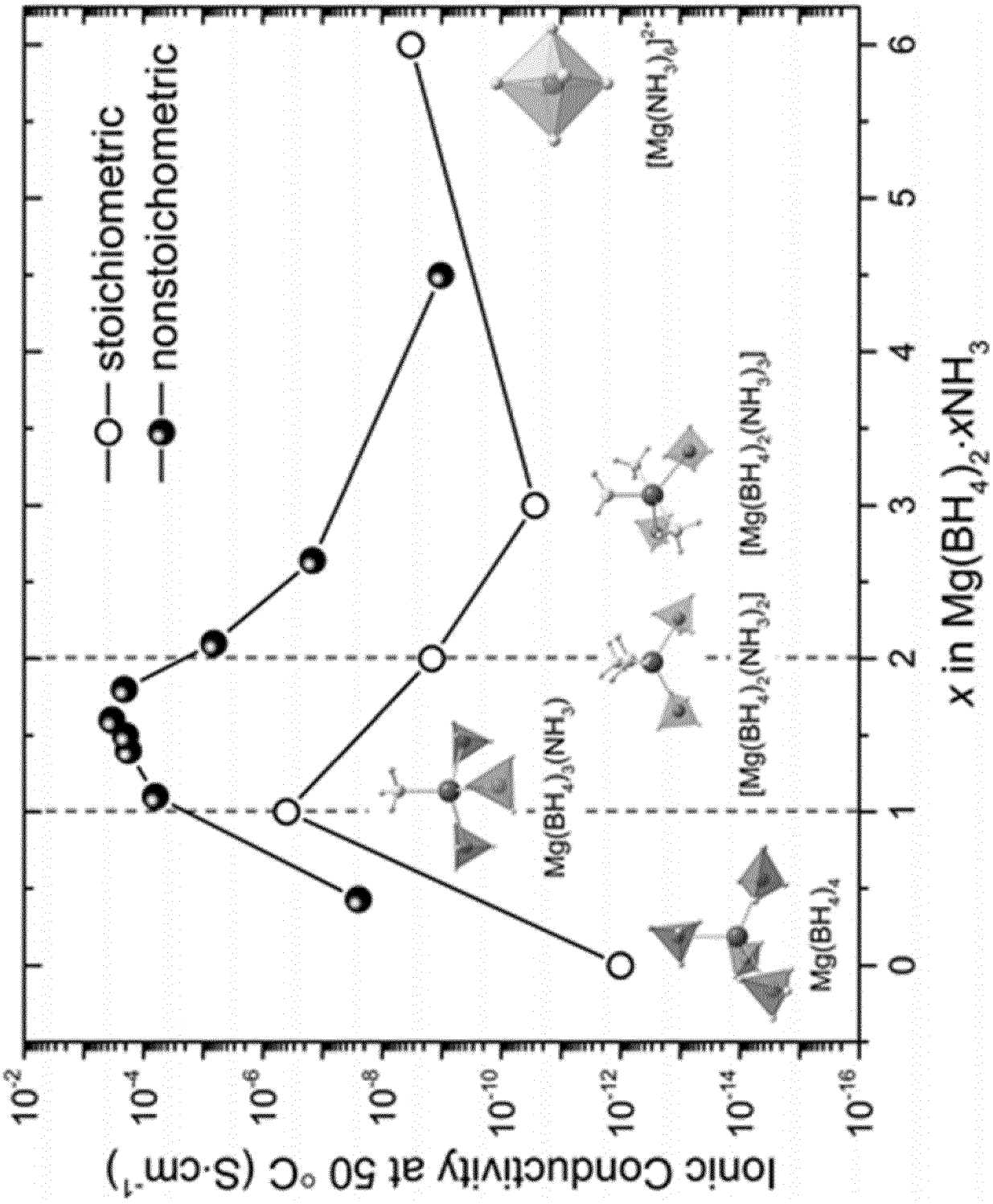
stoichiometric
nonstoichiometric
Ionic Conductivity at 50 °C (S·cm⁻¹)
x in Mg(BH4)2·xNH3
Mg(BH4)4
Mg(BH4)3(NH3)
[Mg(BH4)2(NH3)2]
[Mg(BH4)2(NH3)4]
[Mg(NH3)6]2+

FIG. 1

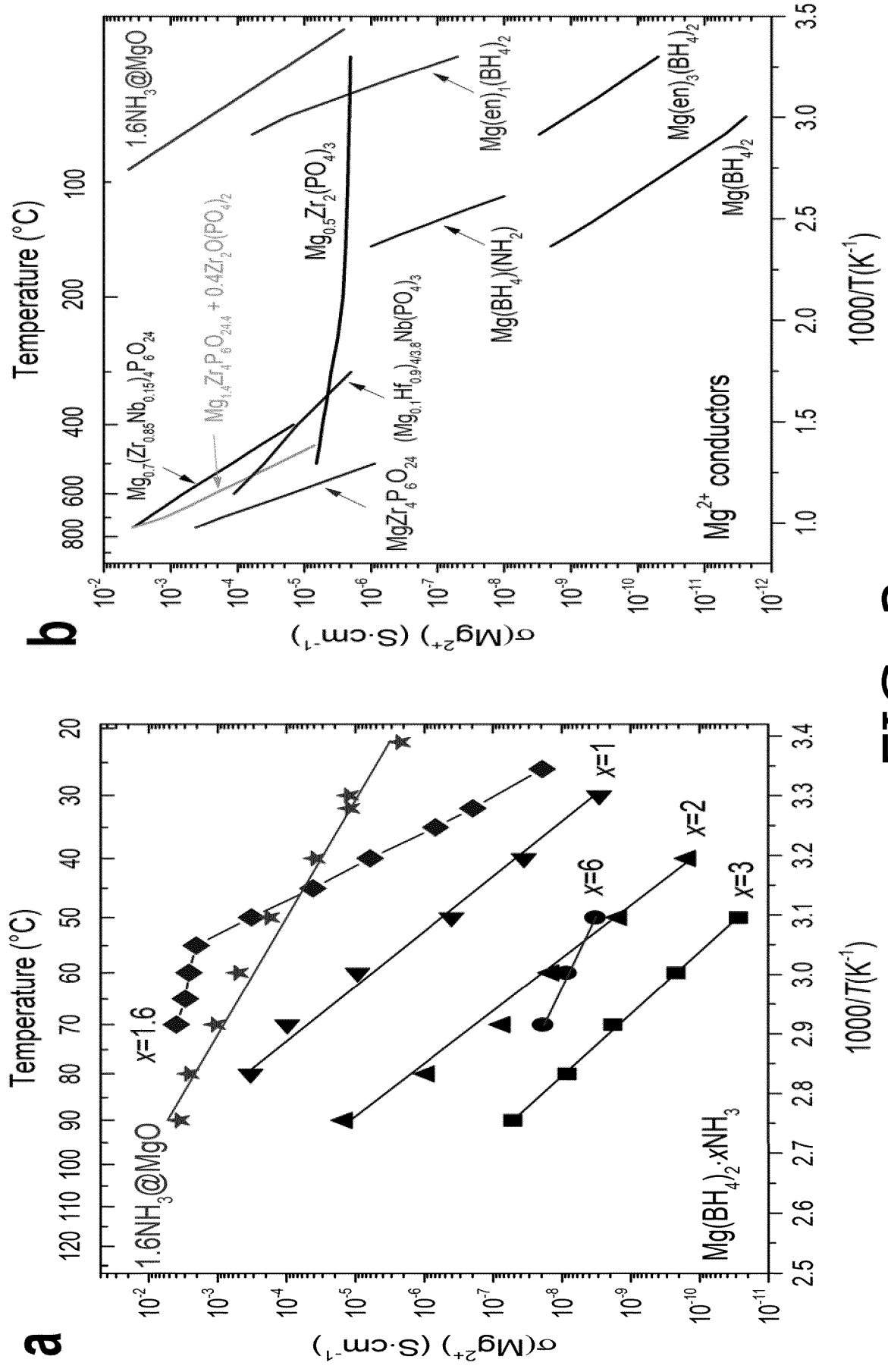
a
Temperature (°C)
1.6NH3@MgO
x=1.6
x=1
x=2
x=6
x=3
Mg(BH4)2·xNH3
σ(Mg2+) (S·cm-1)
1000/T(K-1)
b
Temperature (°C)
1.6NH3@MgO
Mg0.7(Zr0.85Nb0.15)4P6O24
Mg1.4Zr4P6O24.4 + 0.4Zr2O(PO4)2
Mg0.5Zr2(PO4)3
Mg(en)1(BH4)2
Mg(en)3(BH4)2
MgZr4P6O24
(Mg0.1Hf0.9)4/3.8Nb(PO4)3
Mg(BH4)(NH2)
Mg(BH4)2
Mg2+ conductors
σ(Mg2+) (S·cm-1)
1000/T(K-1)

FIG. 2

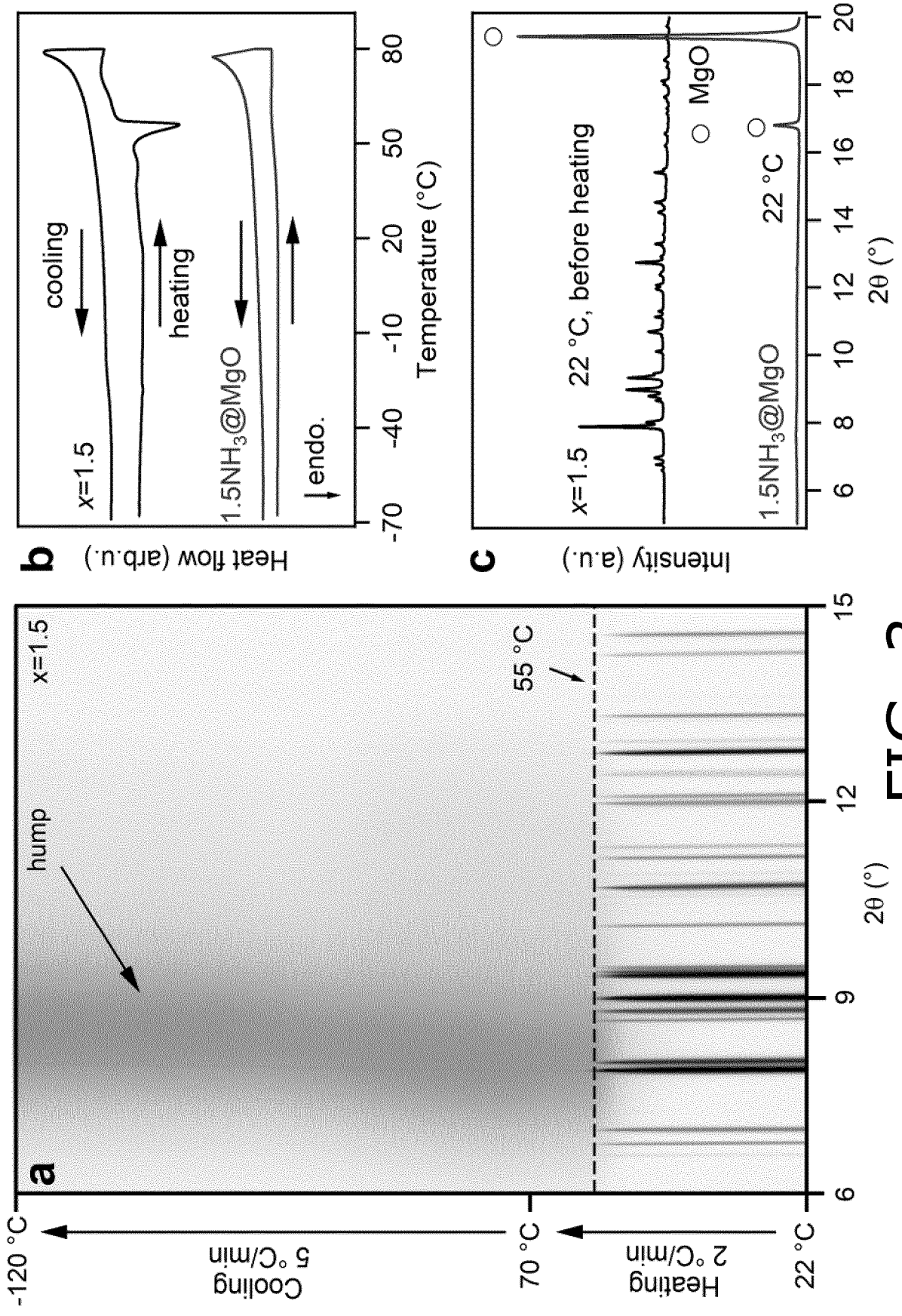
a
x=1.5
hump
55 °C
-120 °C
70 °C
22 °C
Cooling
5 °C/min
Heating
2 °C/min
6
9
12
15
2θ (°)
b
Heat flow (arb.u.)
cooling
heating
x=1.5
1.5NH3@MgO
endo.
-70
-40
-10
20
50
80
Temperature (°C)
c
Intensity (a.u.)
x=1.5
22 °C, before heating
MgO
22 °C
1.5NH3@MgO
6
8
10
12
14
16
18
20
2θ (°)

FIG. 3

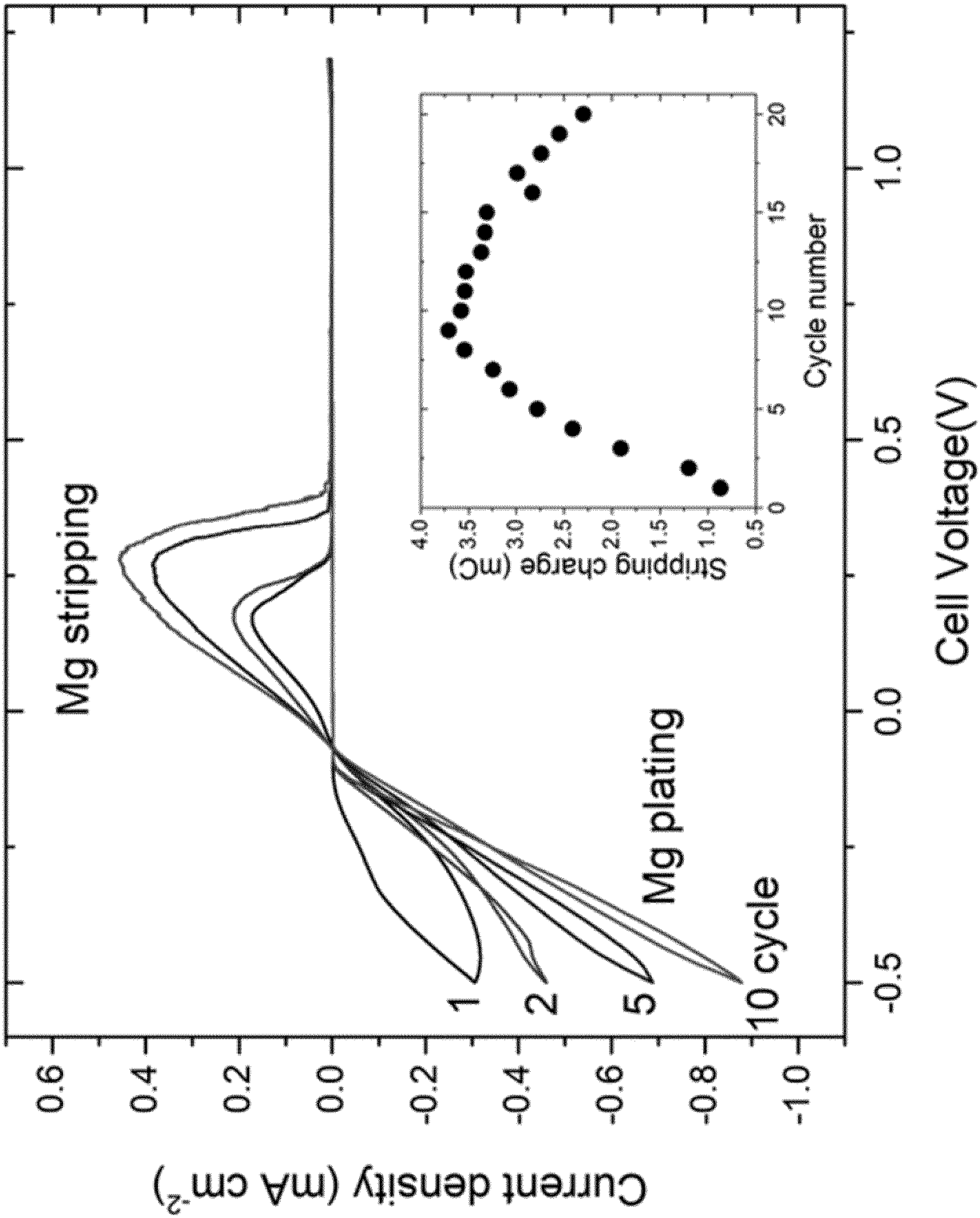
Mg stripping
Mg plating
1
2
5
10 cycle
Current density (mA cm-2)
Cell Voltage(V)
Stripping charge (mC)
Cycle number

FIG. 4

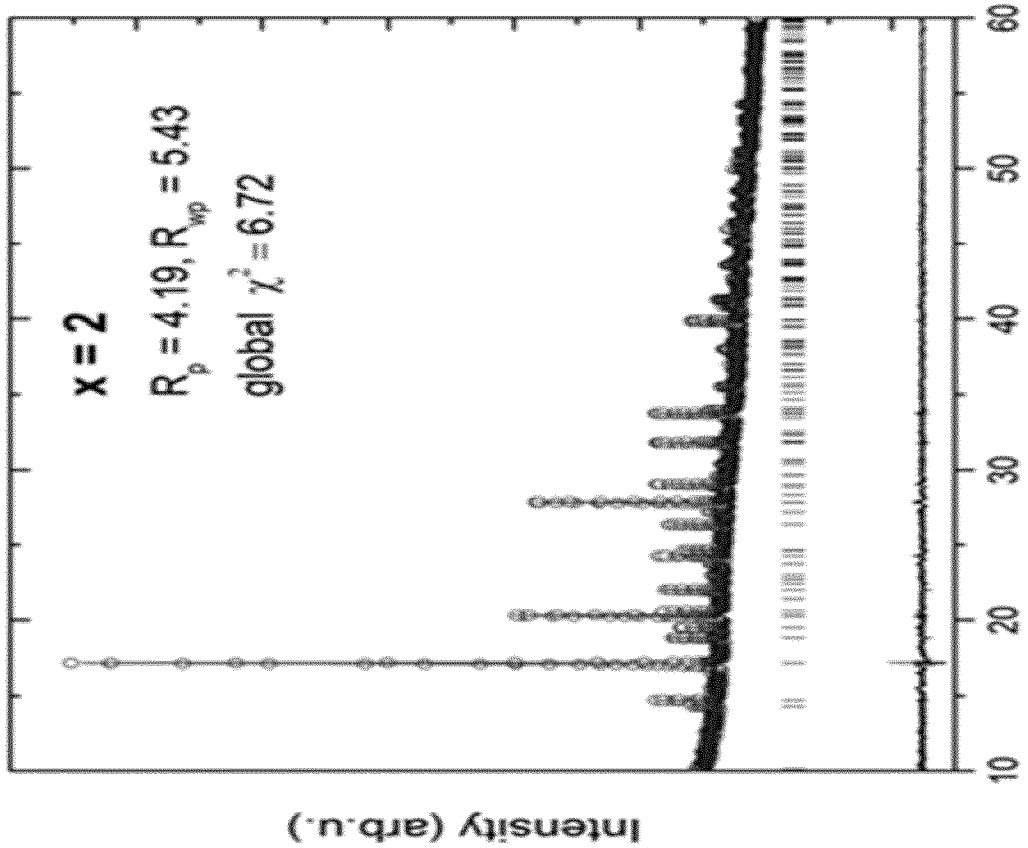
x = 2
$R_p = 4.19, R_{wp} = 5.43$
global $\chi^2 = 6.72$
Intensity (arb.u.)
2θ (°)
10
20
30
40
50
60

FIG. 6

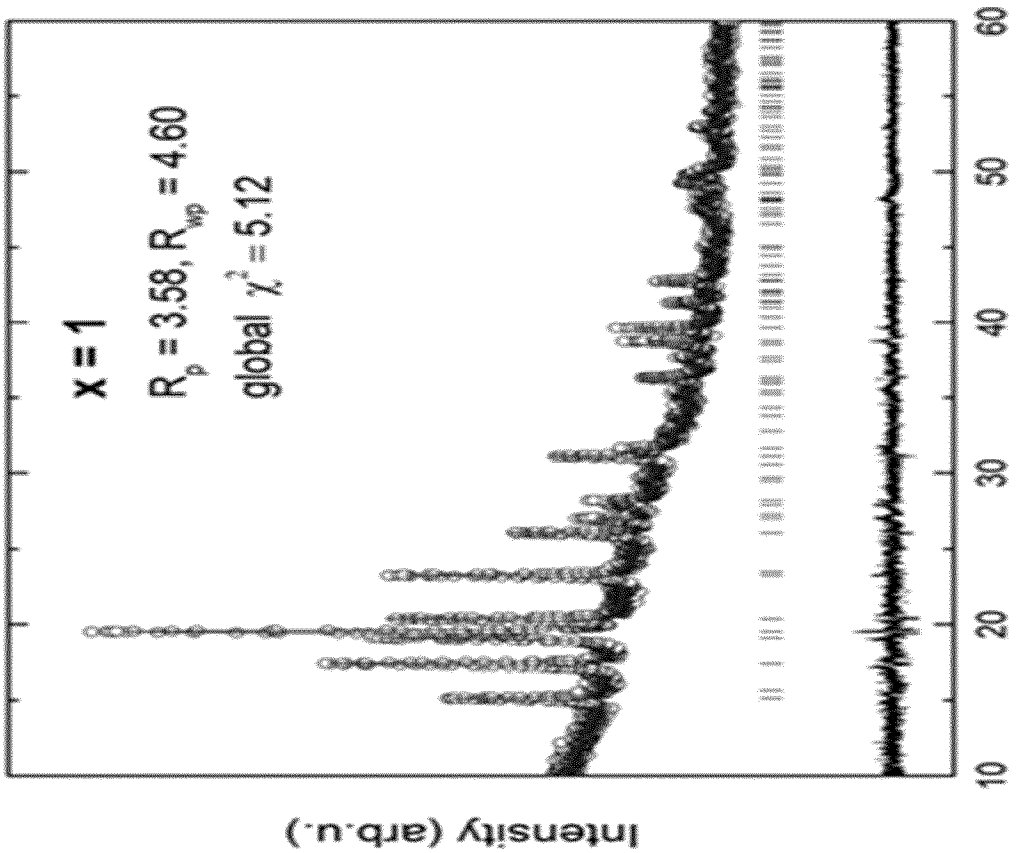
x = 1
$R_p = 3.58, R_{wp} = 4.60$
global $\chi^2 = 5.12$
Intensity (arb.u.)
2θ (°)
10
20
30
40
50
60

FIG. 5

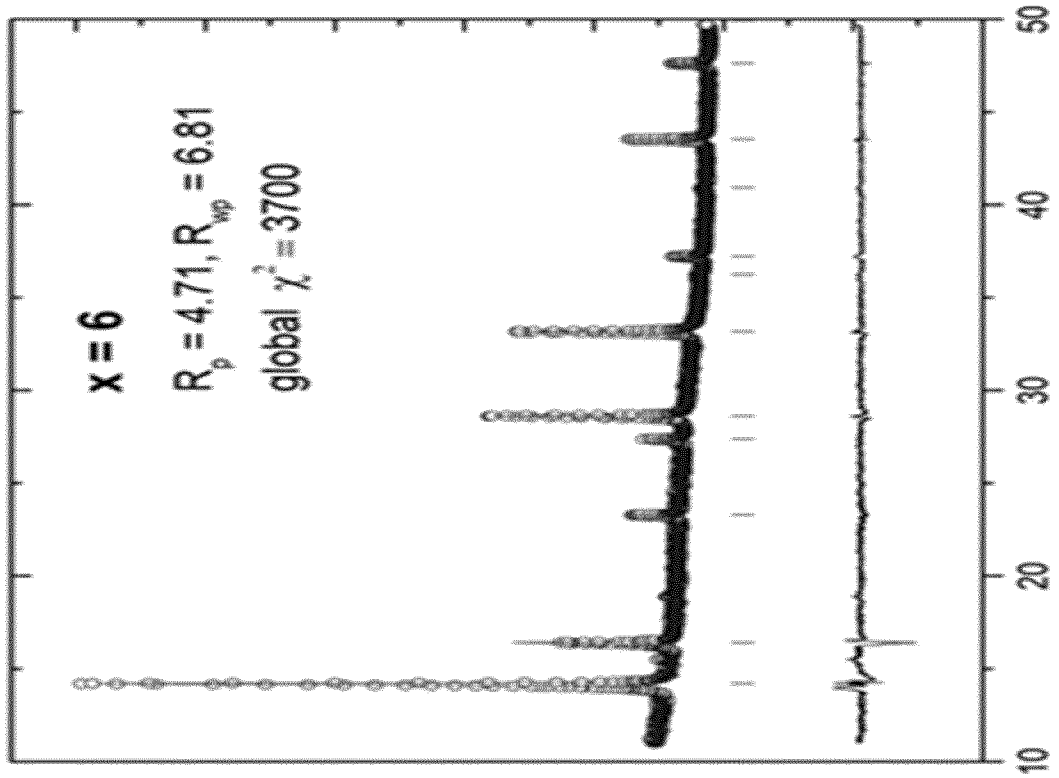
x = 6
$R_p = 4.71, R_{wp} = 6.81$
global $\chi^2 = 3700$
Intensity (arb.u.)
10
20
30
40
50
2θ (°)

FIG. 8

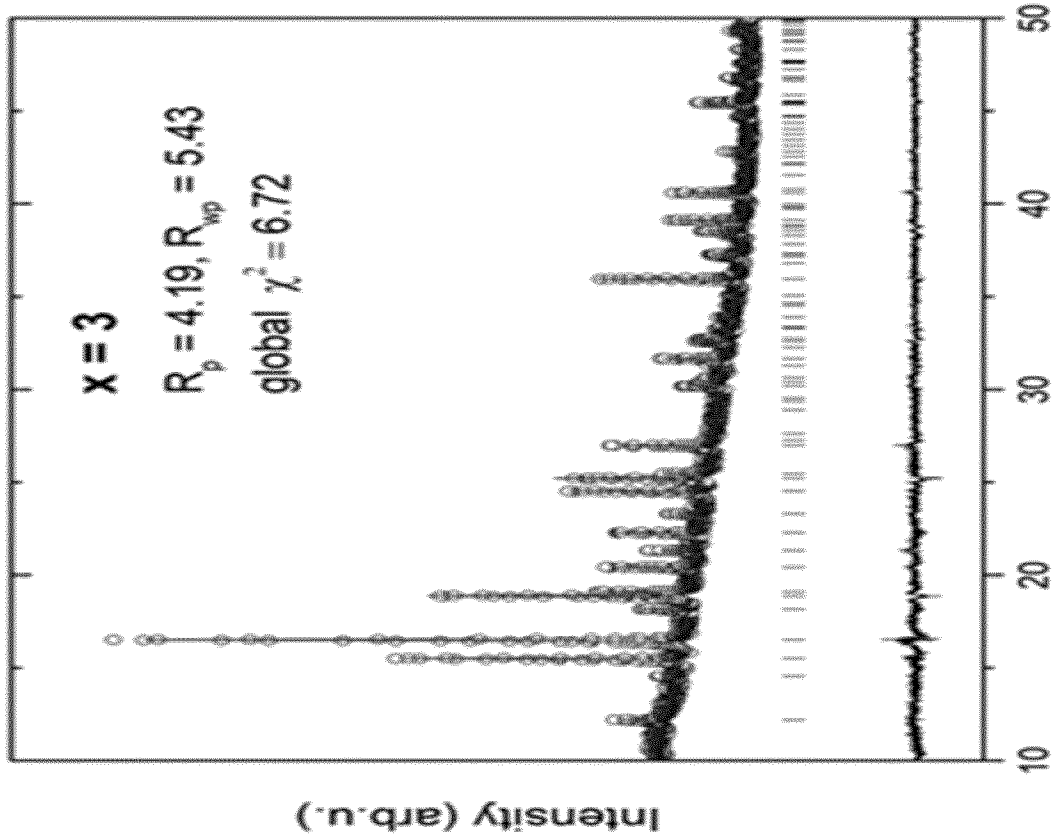
x = 3
$R_p = 4.19, R_{wp} = 5.43$
global $\chi^2 = 6.72$
Intensity (arb.u.)
10
20
30
40
50
2θ (°)

FIG. 7

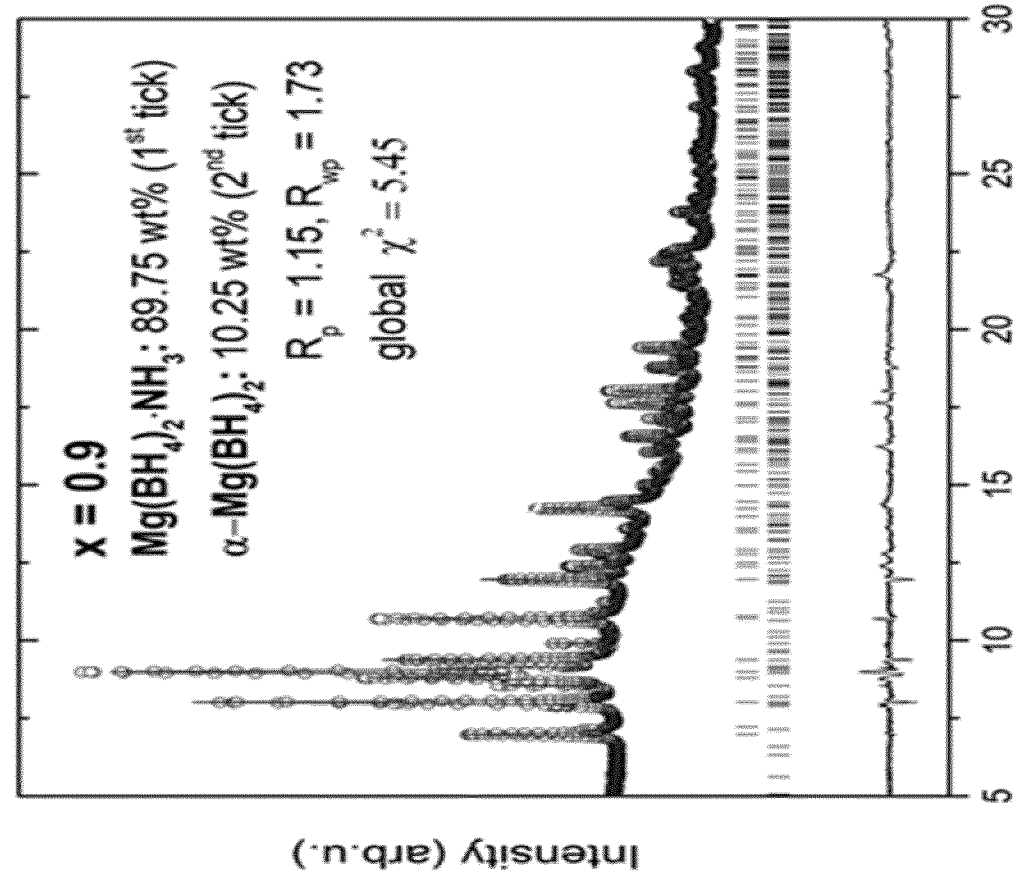
x = 0.9
$Mg(BH_4)_2 \cdot NH_3$: 89.75 wt% (1st tick)
α–$Mg(BH_4)_2$: 10.25 wt% (2nd tick)
R_p = 1.15, R_{wp} = 1.73
global χ^2 = 5.45
Intensity (arb.u.)
2θ (°)
5
10
15
20
25
30

FIG. 10

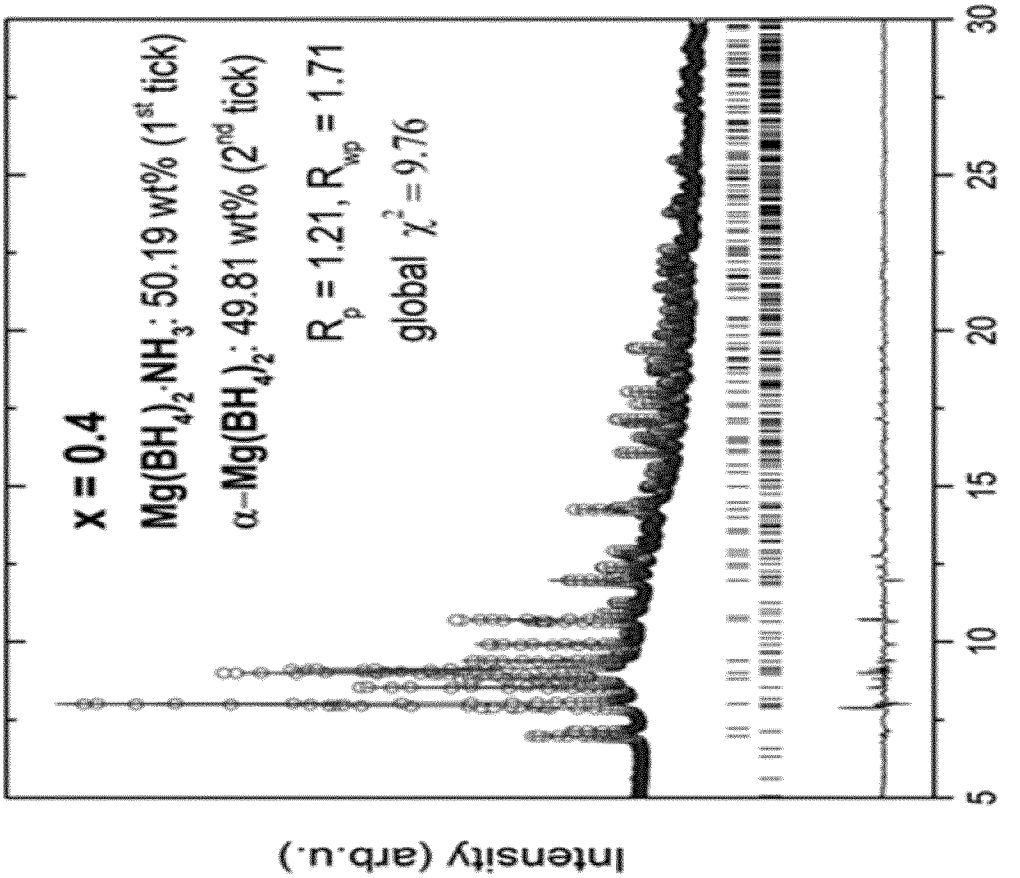
x = 0.4
$Mg(BH_4)_2 \cdot NH_3$: 50.19 wt% (1st tick)
α–$Mg(BH_4)_2$: 49.81 wt% (2nd tick)
R_p = 1.21, R_{wp} = 1.71
global χ^2 = 9.76
Intensity (arb.u.)
2θ (°)
5
10
15
20
25
30

FIG. 9

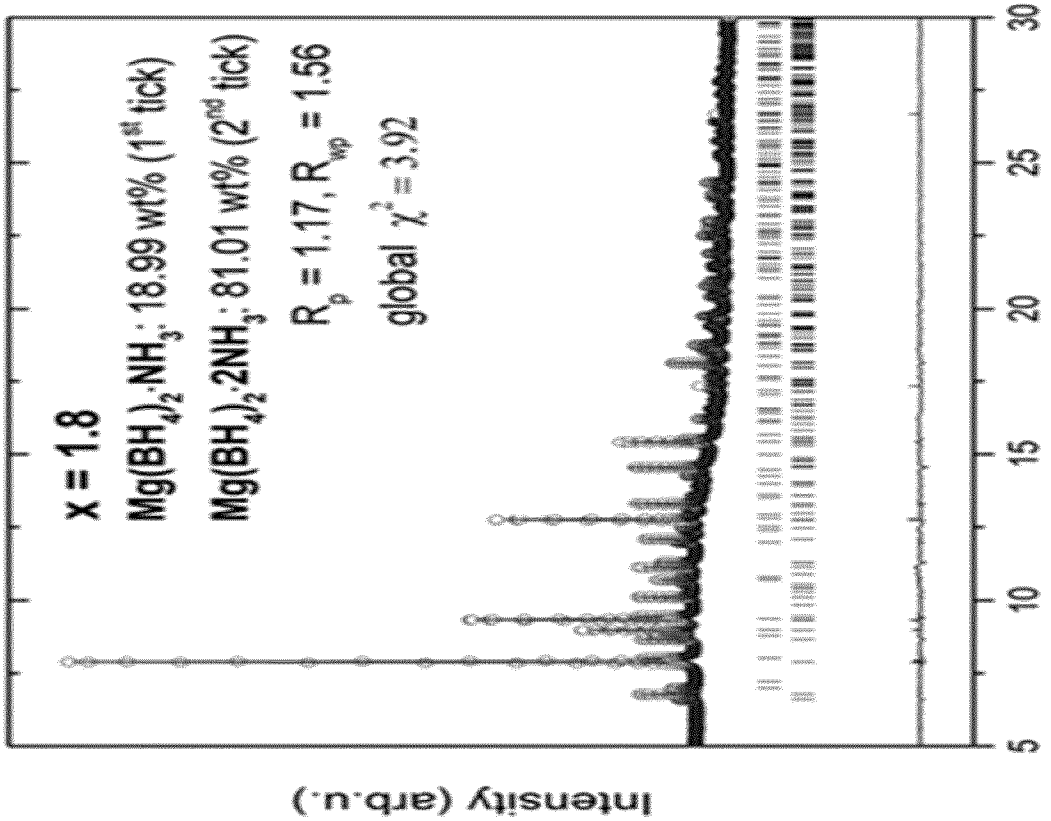
x = 1.8
$Mg(BH_4)_2 \cdot NH_3$: 18.99 wt% (1st tick)
$Mg(BH_4)_2 \cdot 2NH_3$: 81.01 wt% (2nd tick)
$R_p = 1.17, R_{wp} = 1.56$
global $\chi^2 = 3.92$
Intensity (arb.u.)
2θ (°)
5
10
15
20
25
30

FIG. 12

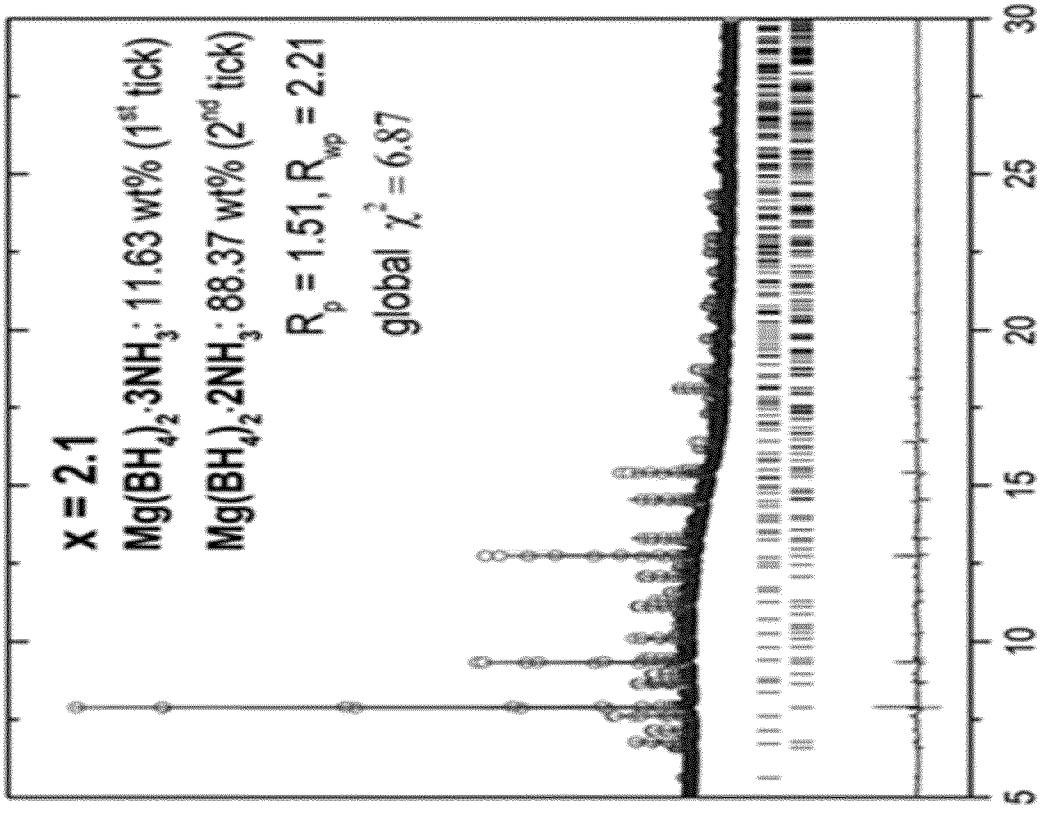
x = 2.1
$Mg(BH_4)_2 \cdot 3NH_3$: 11.63 wt% (1st tick)
$Mg(BH_4)_2 \cdot 2NH_3$: 88.37 wt% (2nd tick)
$R_p = 1.51, R_{wp} = 2.21$
global $\chi^2 = 6.87$
Intensity (arb.u.)
2θ (°)
5
10
15
20
25
30

FIG. 11

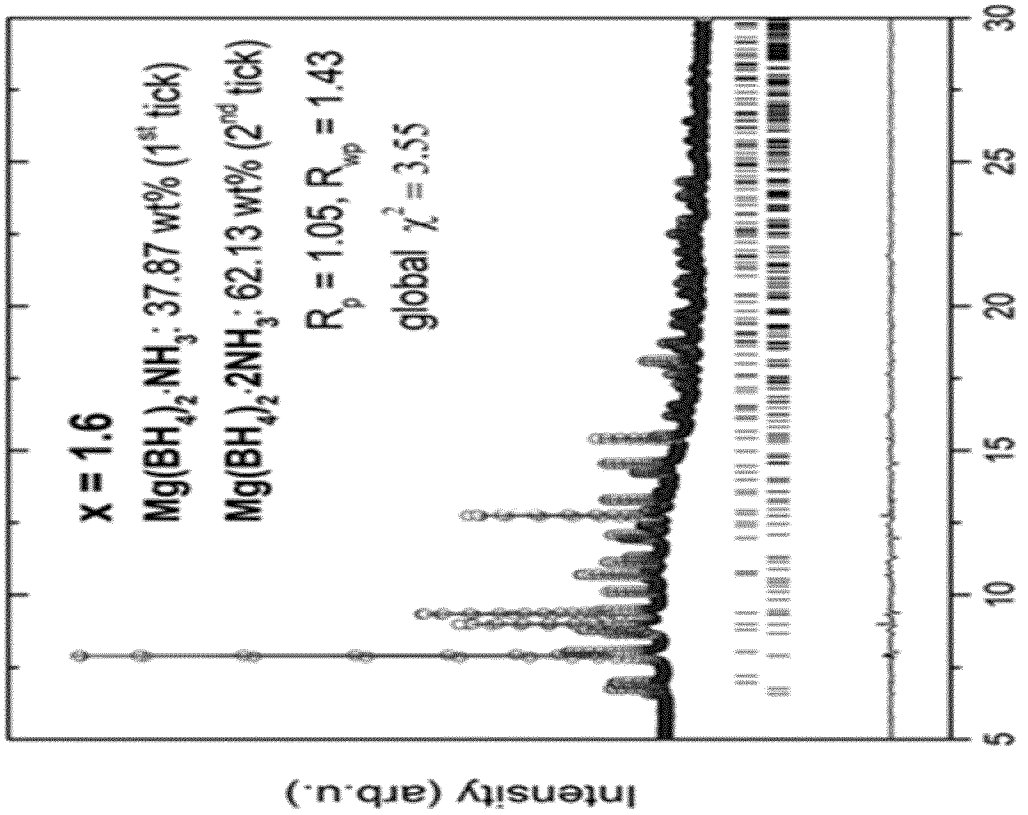
x = 1.6
Mg(BH4)2·NH3: 37.87 wt% (1st tick)
Mg(BH4)2·2NH3: 62.13 wt% (2nd tick)
Rp = 1.05, Rwp = 1.43
global χ2 = 3.55
Intensity (arb.u.)
2θ (°)
5
10
15
20
25
30

FIG. 14

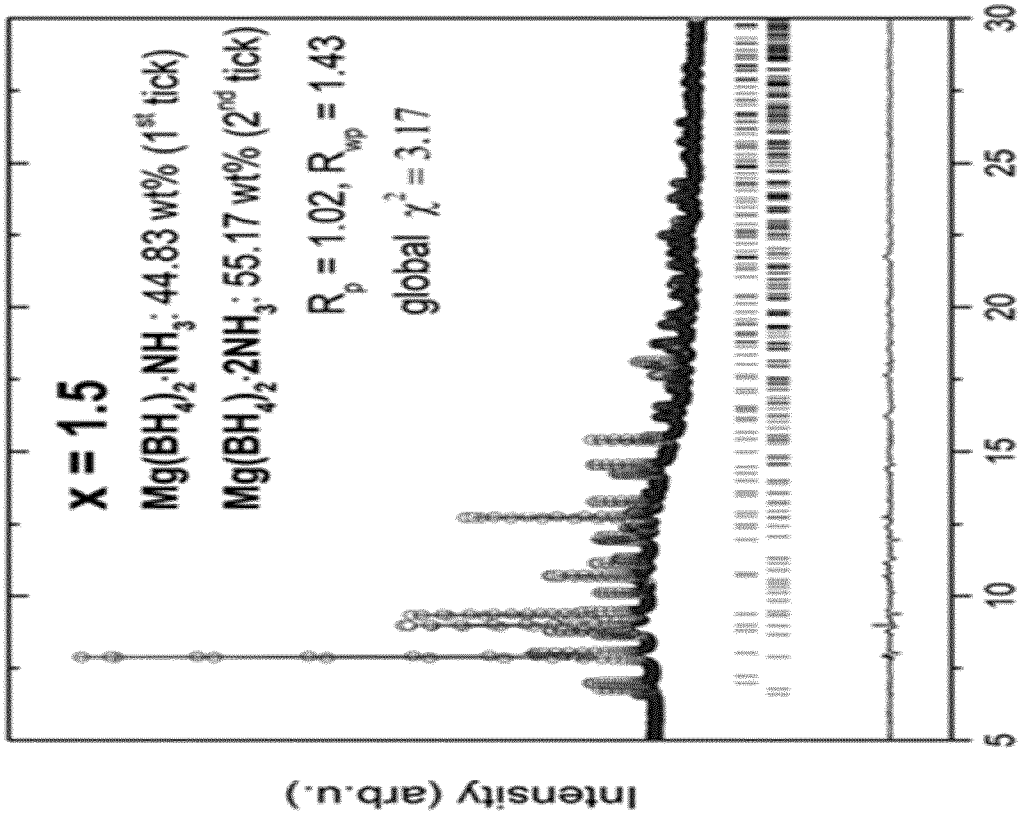
x = 1.5
Mg(BH4)2·NH3: 44.83 wt% (1st tick)
Mg(BH4)2·2NH3: 55.17 wt% (2nd tick)
Rp = 1.02, Rwp = 1.43
global χ2 = 3.17
Intensity (arb.u.)
2θ (°)
5
10
15
20
25
30

FIG. 13

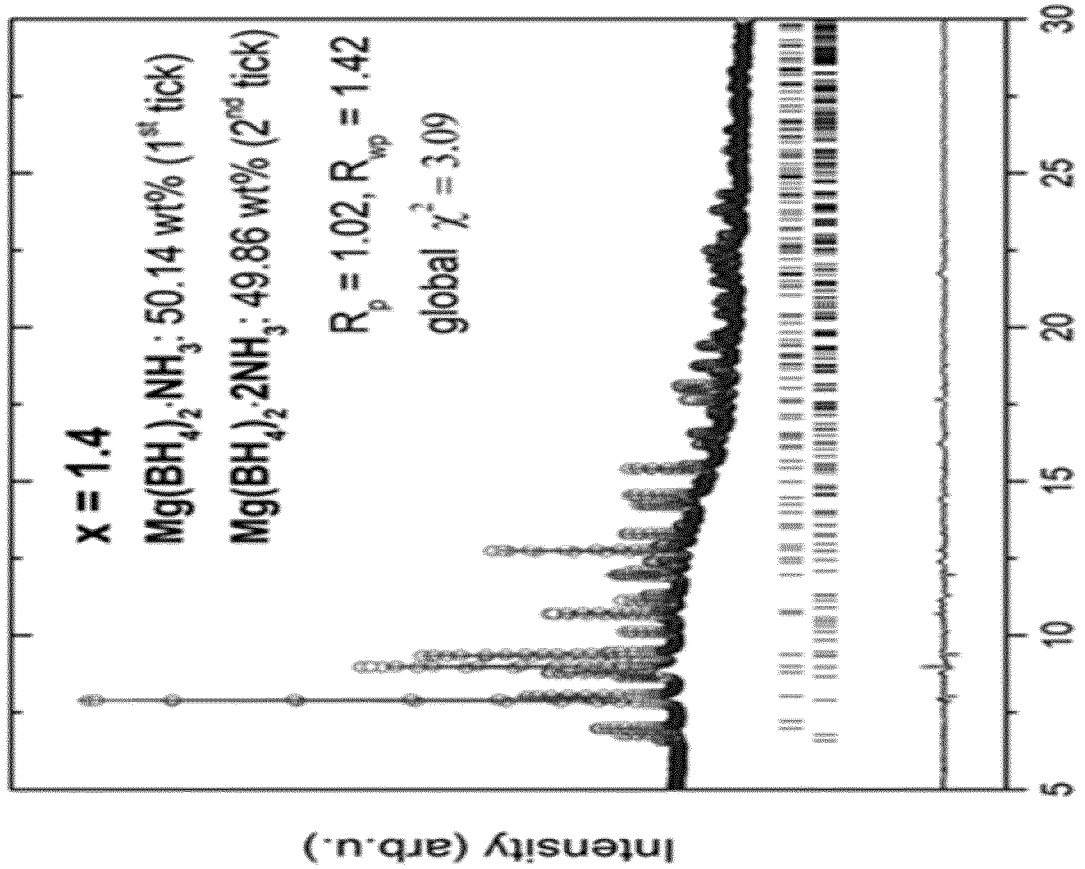
x = 1.4
Mg(BH4)2·NH3: 50.14 wt% (1st tick)
Mg(BH4)2·2NH3: 49.86 wt% (2nd tick)
Rp = 1.02, Rwp = 1.42
global χ2 = 3.09
Intensity (arb.u.)
2θ (°)
5
10
15
20
25
30

FIG. 16

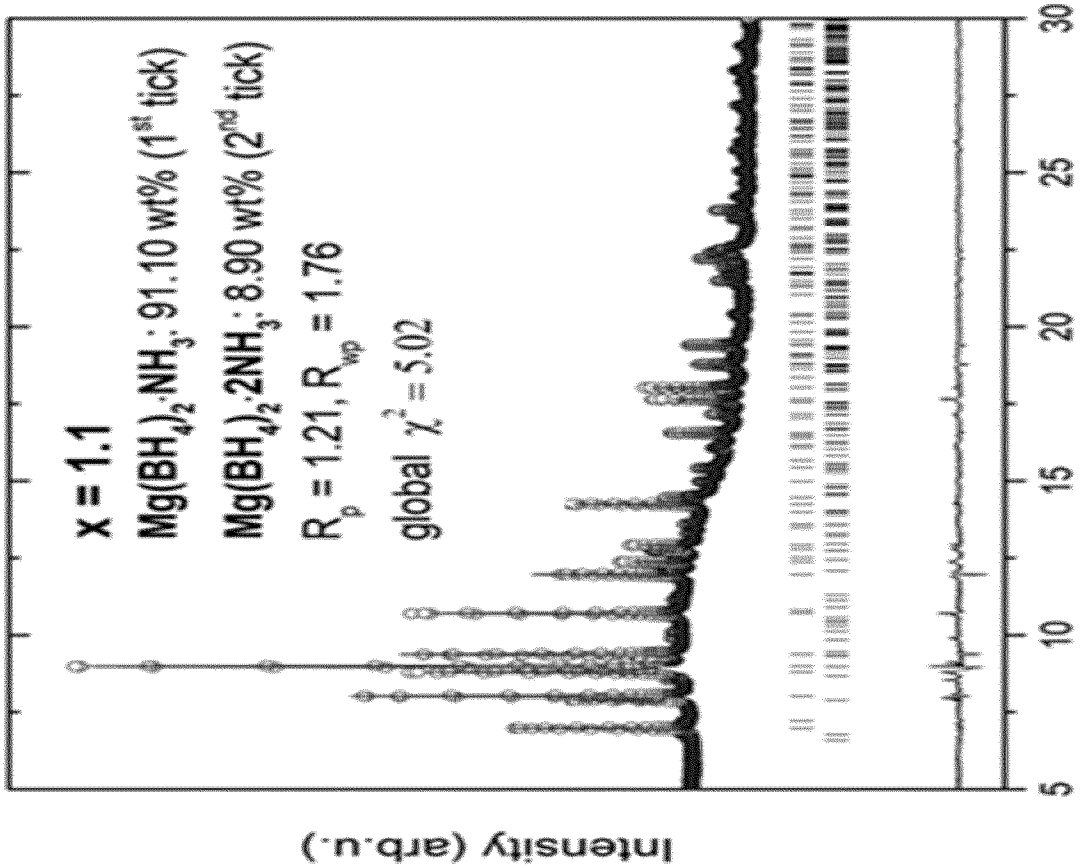
x = 1.1
Mg(BH4)2·NH3: 91.10 wt% (1st tick)
Mg(BH4)2·2NH3: 8.90 wt% (2nd tick)
Rp = 1.21, Rwp = 1.76
global χ2 = 5.02
Intensity (arb.u.)
2θ (°)
5
10
15
20
25
30

FIG. 15

FIG. 17

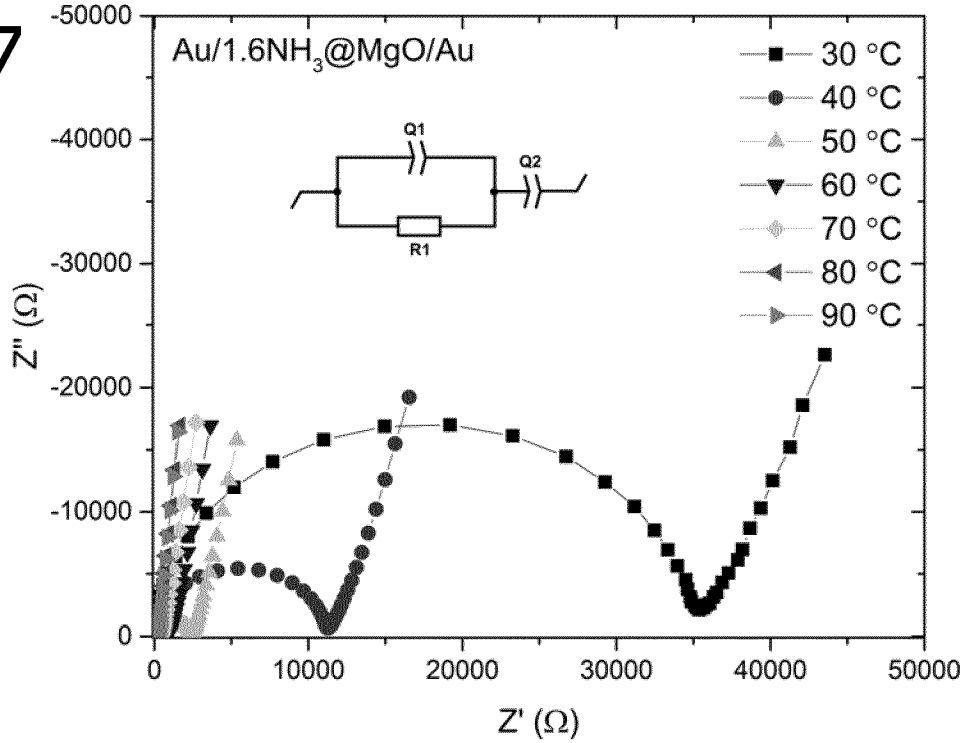
Au/1.6NH3@MgO/Au
30 °C
40 °C
50 °C
60 °C
70 °C
80 °C
90 °C
Q1
Q2
R1
Z'' (Ω)
Z' (Ω)
-50000
-40000
-30000
-20000
-10000
0
0
10000
20000
30000
40000
50000

FIG. 18

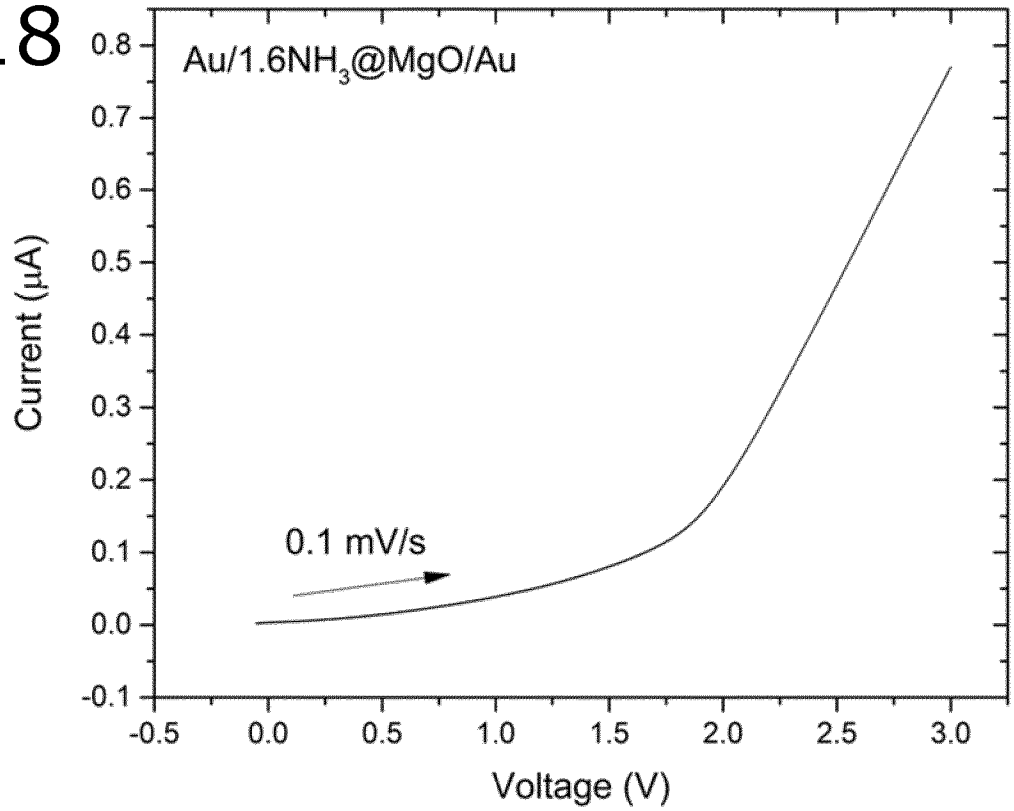
Au/1.6NH3@MgO/Au
0.1 mV/s
Current (μA)
Voltage (V)
0.8
0.7
0.6
0.5
0.4
0.3
0.2
0.1
0.0
-0.1
-0.5
0.0
0.5
1.0
1.5
2.0
2.5
3.0

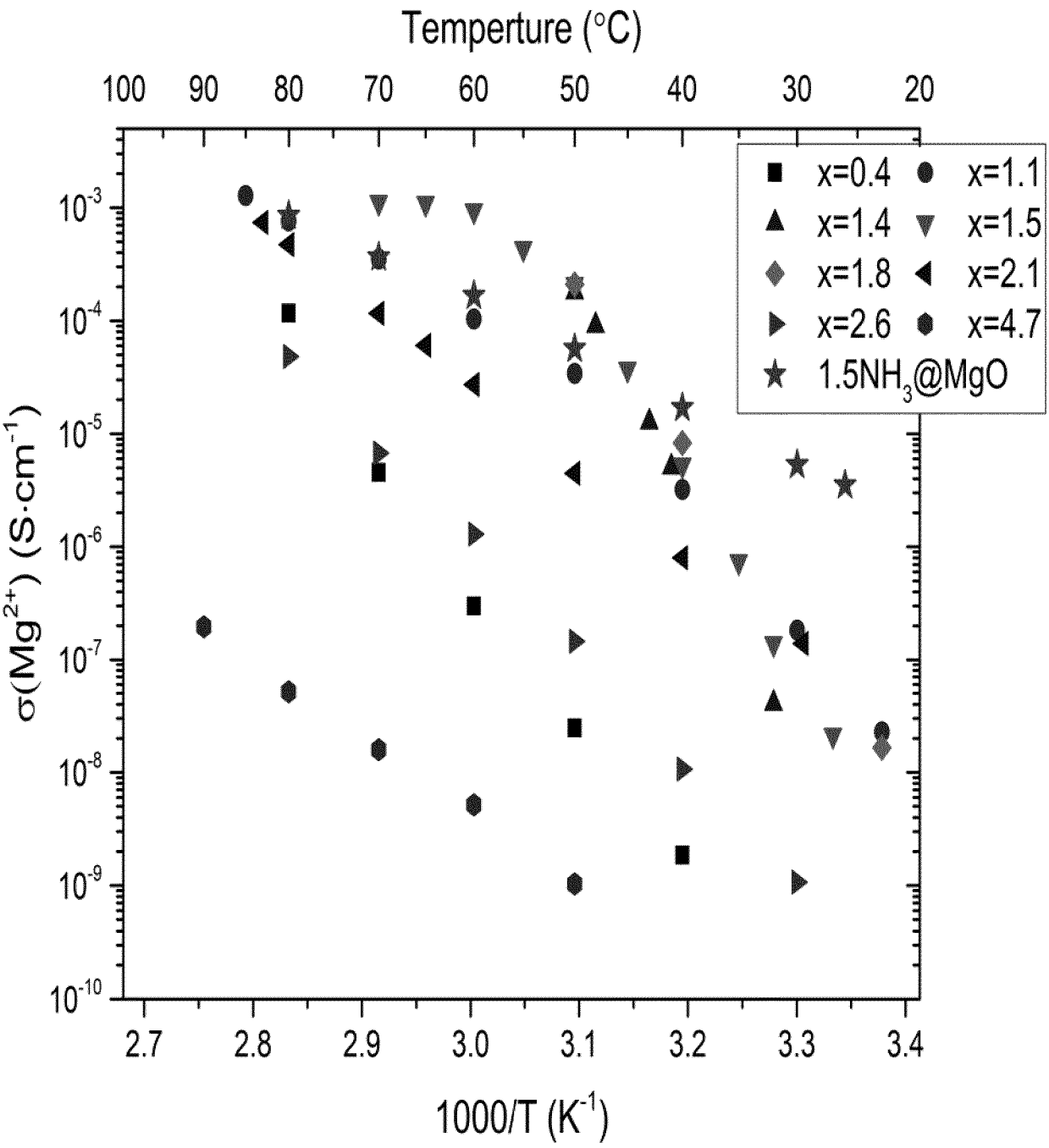
Temperture (°C)
100
90
80
70
60
50
40
30
20
x=0.4
x=1.1
x=1.4
x=1.5
x=1.8
x=2.1
x=2.6
x=4.7
1.5NH3@MgO
σ(Mg2+) (S·cm-1)
10-3
10-4
10-5
10-6
10-7
10-8
10-9
10-10
2.7
2.8
2.9
3.0
3.1
3.2
3.3
3.4
1000/T (K-1)

FIG. 19

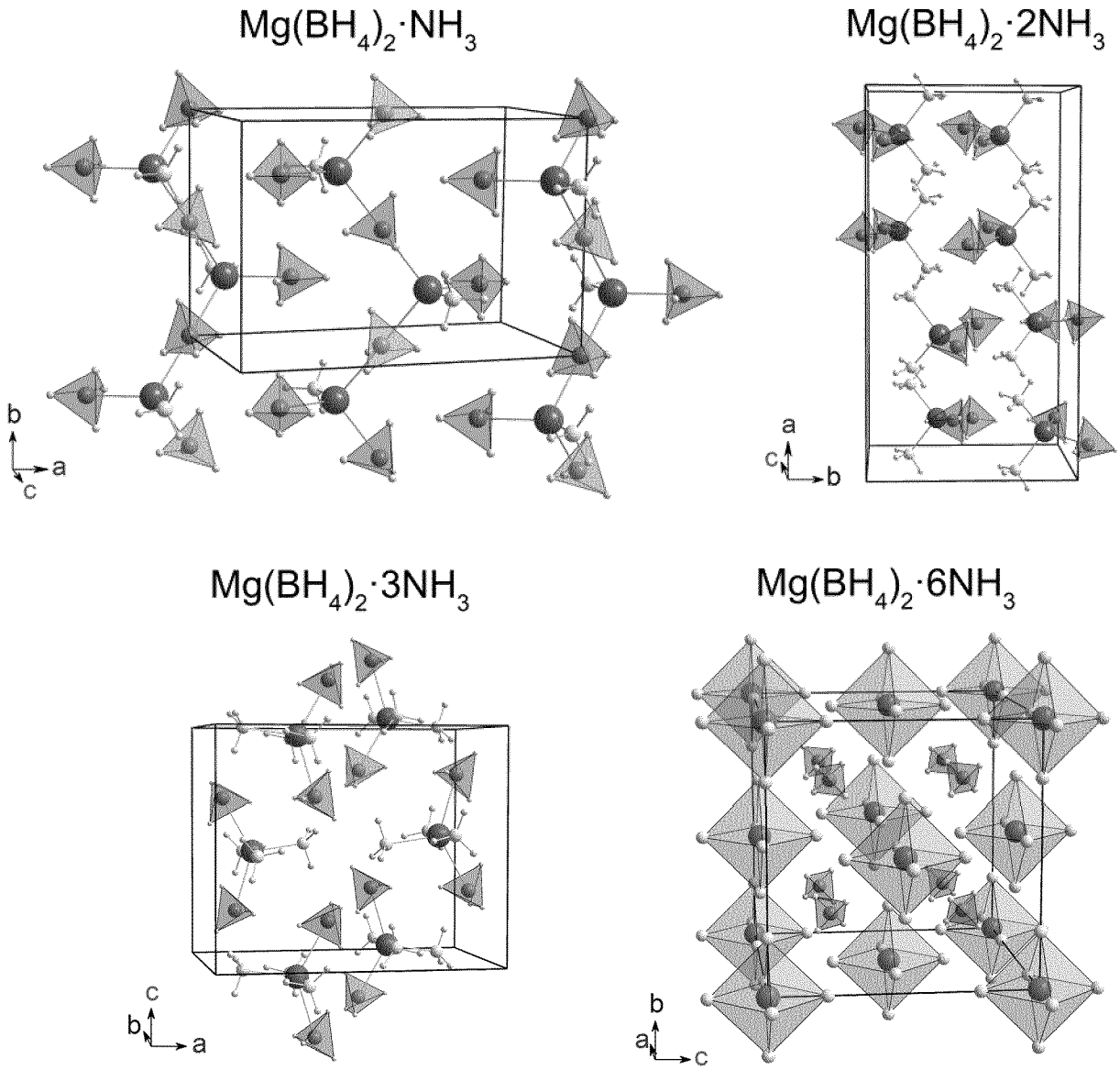
$Mg(BH_4)_2 \cdot NH_3$
$Mg(BH_4)_2 \cdot 2NH_3$
$Mg(BH_4)_2 \cdot 3NH_3$
$Mg(BH_4)_2 \cdot 6NH_3$
b
a
c
a
c
b
c
b
a
b
a
c

FIG. 20

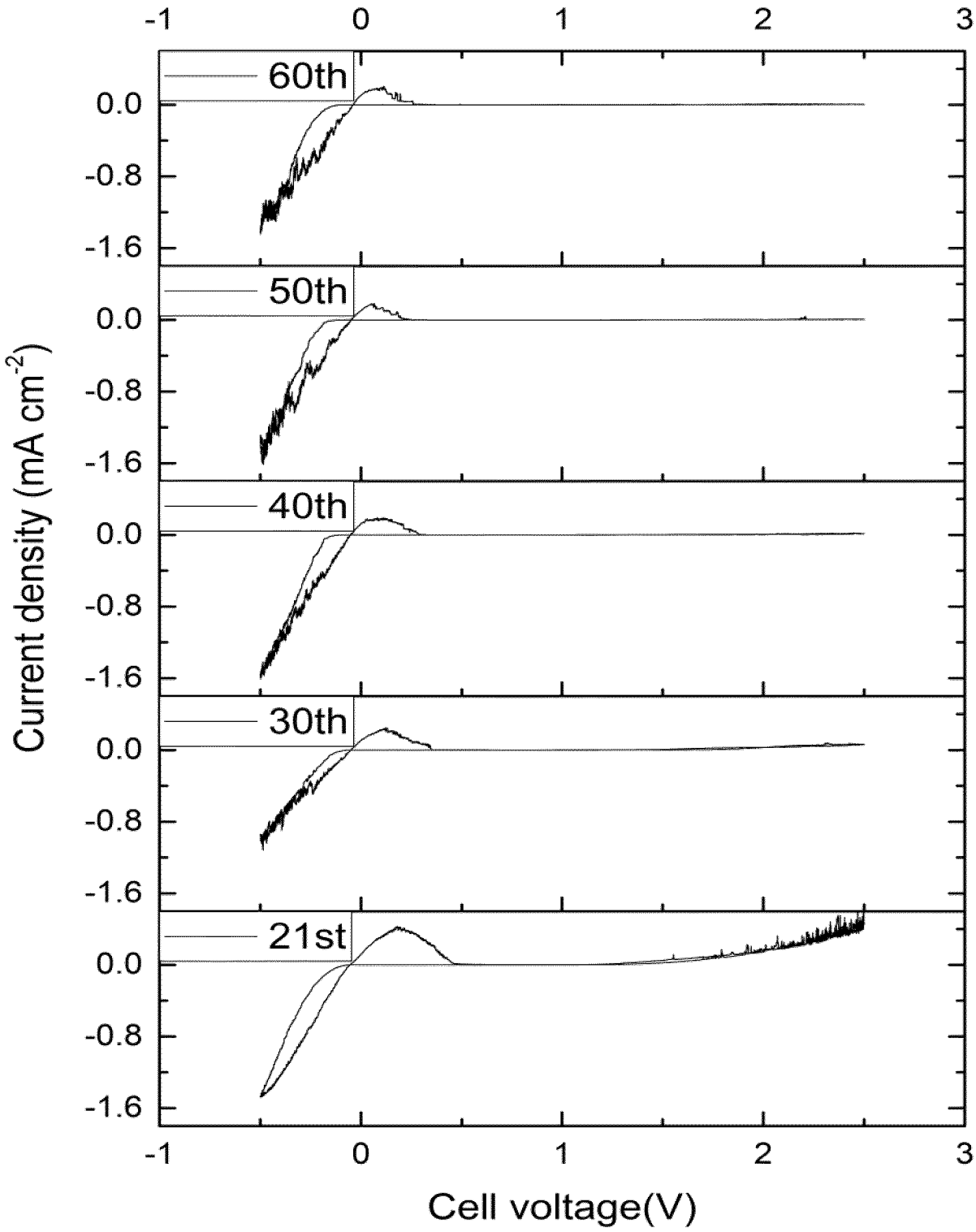
60th
50th
40th
30th
21st
Current density (mA cm-2)
Cell voltage(V)
-1
0
1
2
3
0.0
-0.8
-1.6

FIG. 21

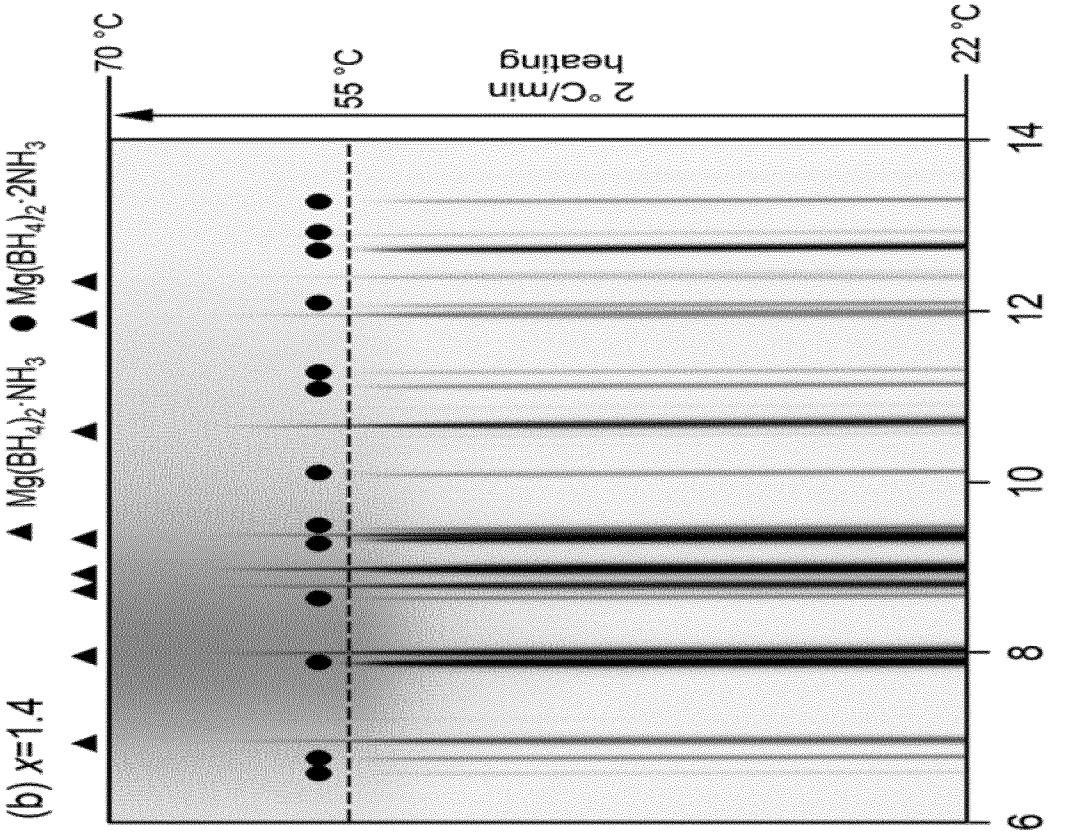
(b) x=1.4
▲ $Mg(BH_4)_2 \cdot NH_3$ ● $Mg(BH_4)_2 \cdot 2NH_3$
70 °C
55 °C
22 °C
2 °C/min heating
6
8
10
12
14
2θ (°)

FIG. 23

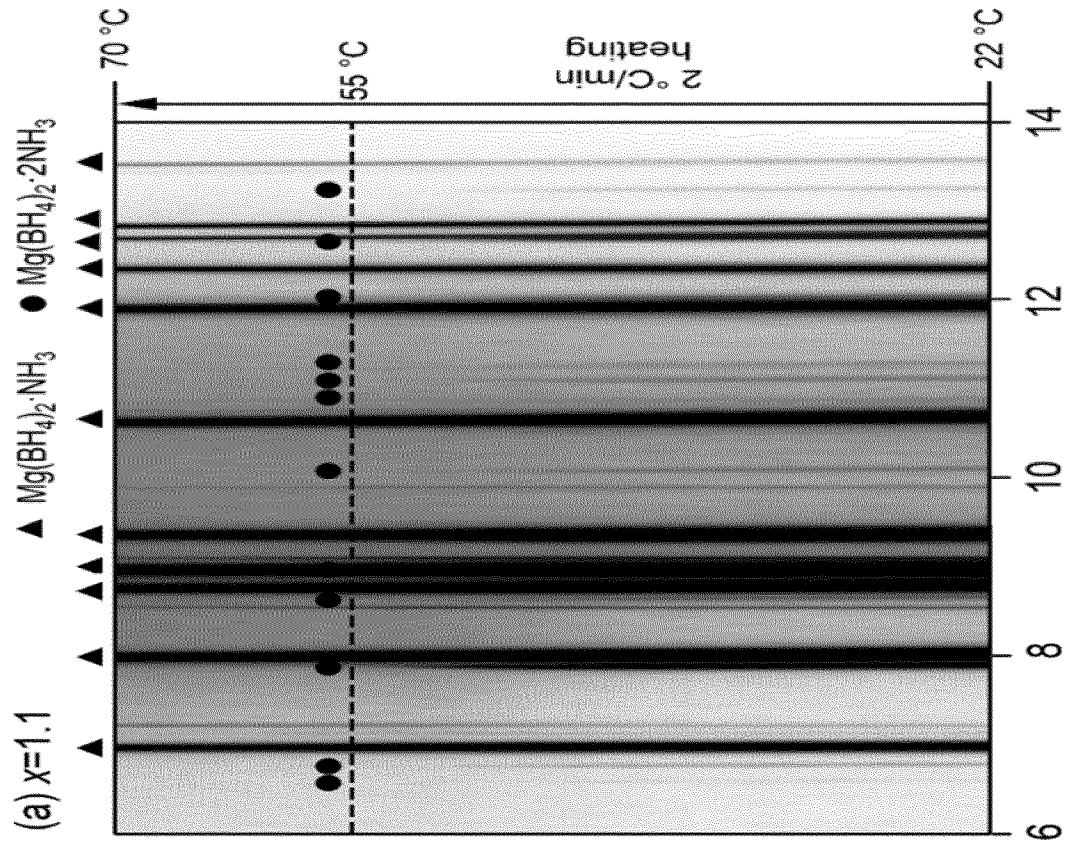
(a) x=1.1
▲ $Mg(BH_4)_2 \cdot NH_3$ ● $Mg(BH_4)_2 \cdot 2NH_3$
70 °C
55 °C
22 °C
2 °C/min heating
6
8
10
12
14
2θ (°)

FIG. 22

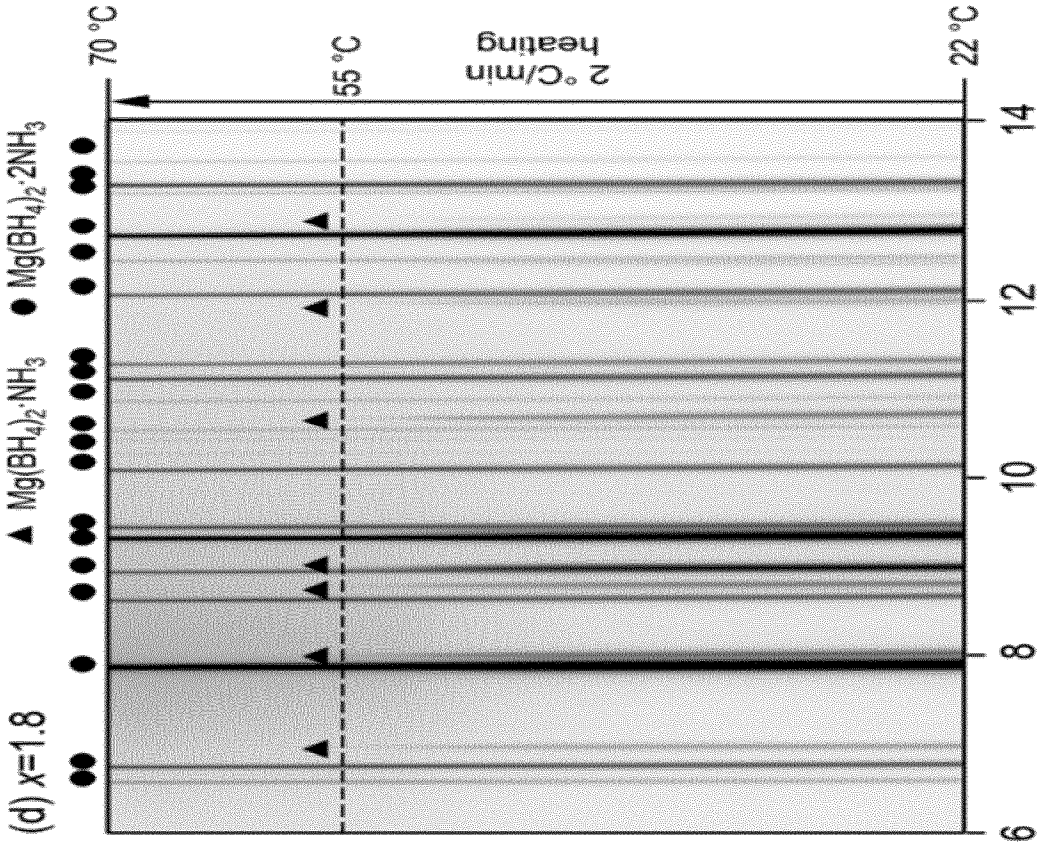
(d) x=1.8
▲ Mg(BH4)2·NH3
● Mg(BH4)2·2NH3
70 °C
55 °C
22 °C
2 °C/min heating
6
8
10
12
14
2θ (°)

FIG. 25

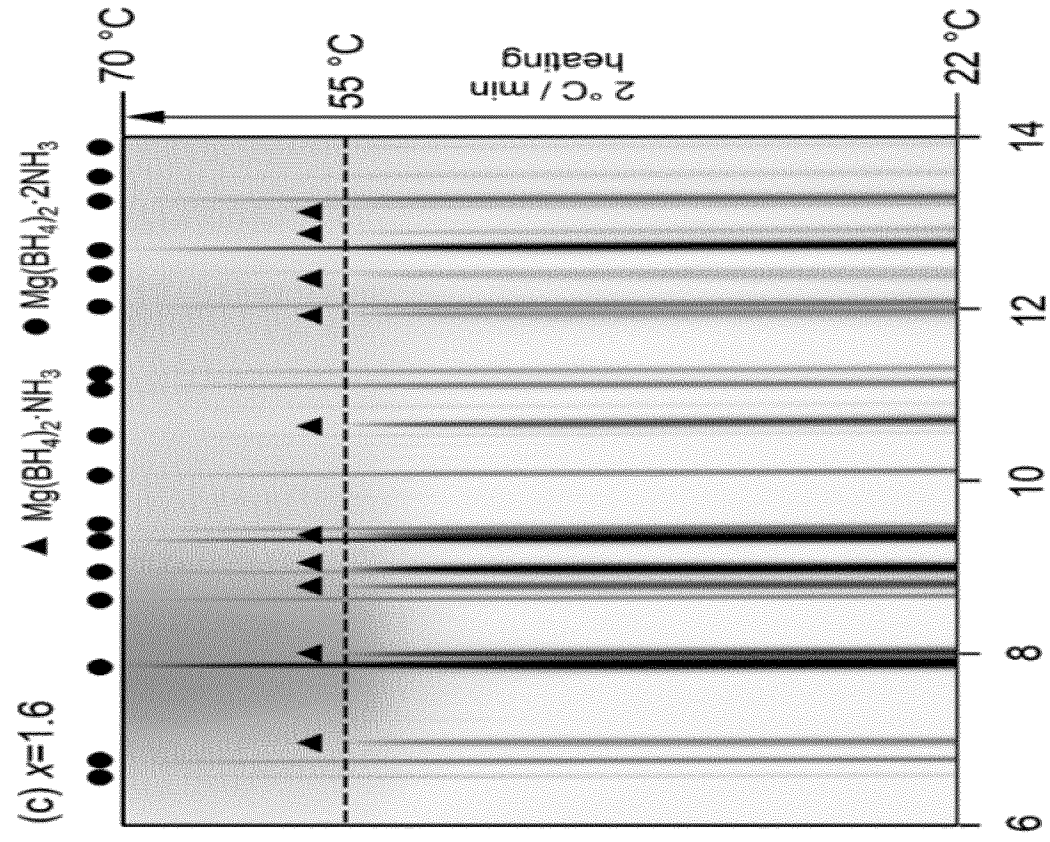
(c) x=1.6
▲ Mg(BH4)2·NH3
● Mg(BH4)2·2NH3
70 °C
55 °C
22 °C
2 °C / min heating
6
8
10
12
14
2θ (°)

FIG. 24

FIG. 26

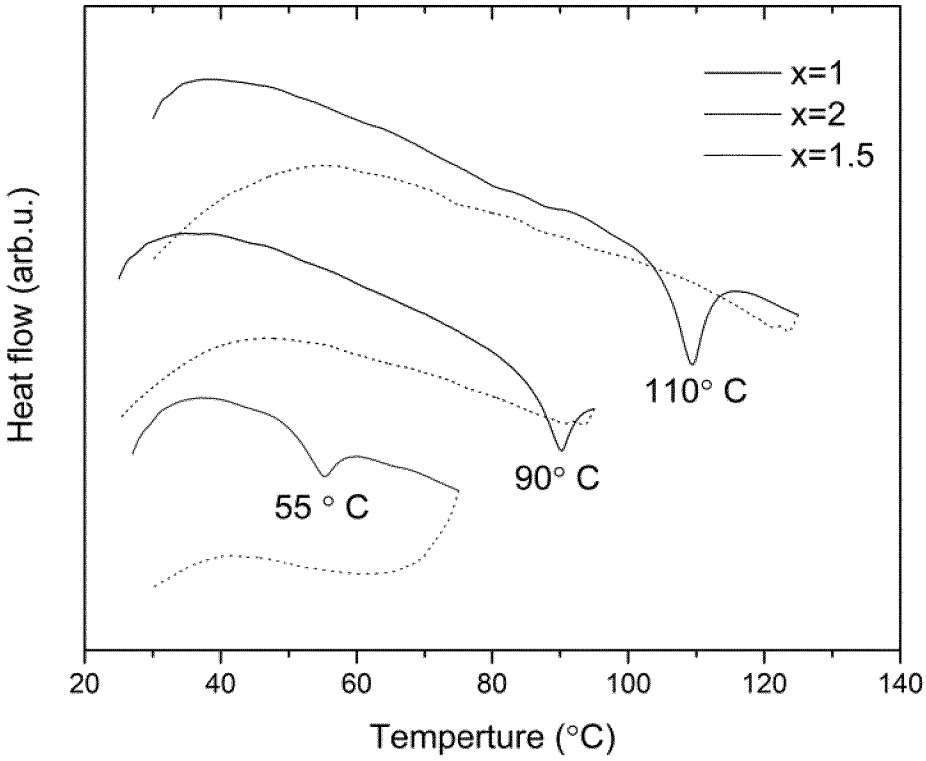
x=1
x=2
x=1.5
110° C
90° C
55 ° C
Heat flow (arb.u.)
20
40
60
80
100
120
140
Temperture (°C)

FIG. 27

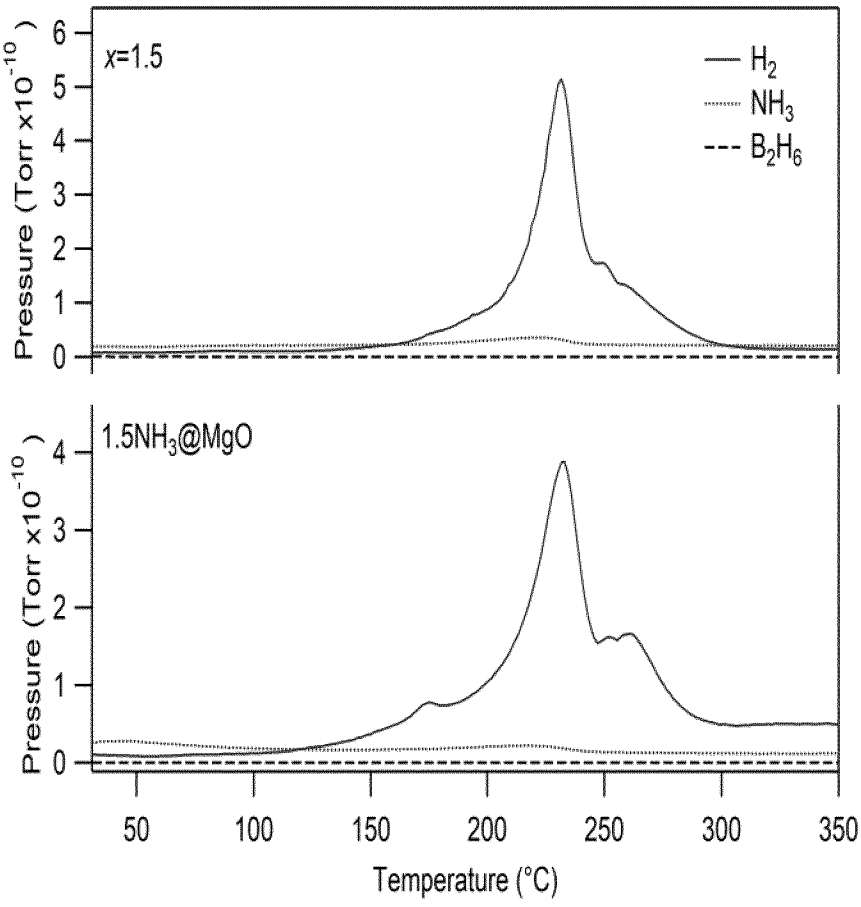
x=1.5
H2
NH3
B2H6
Pressure (Torr x10-10)
0
1
2
3
4
5
6
1.5NH3@MgO
Pressure (Torr x10-10)
0
1
2
3
4
50
100
150
200
250
300
350
Temperature (°C)

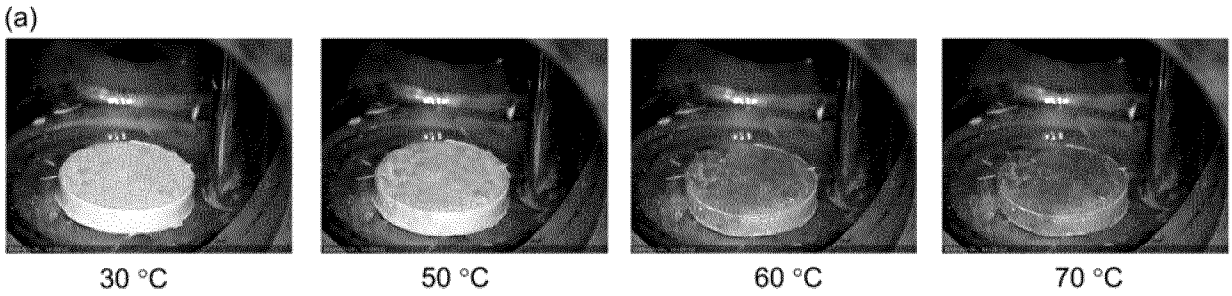

FIG. 28

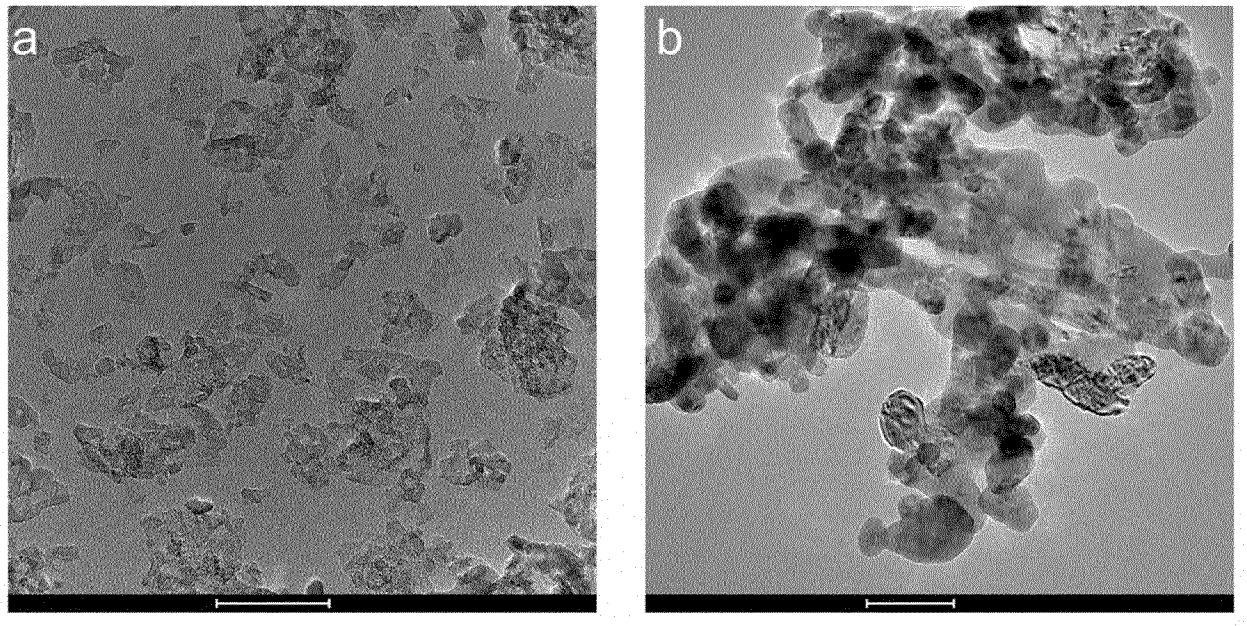

FIG. 29

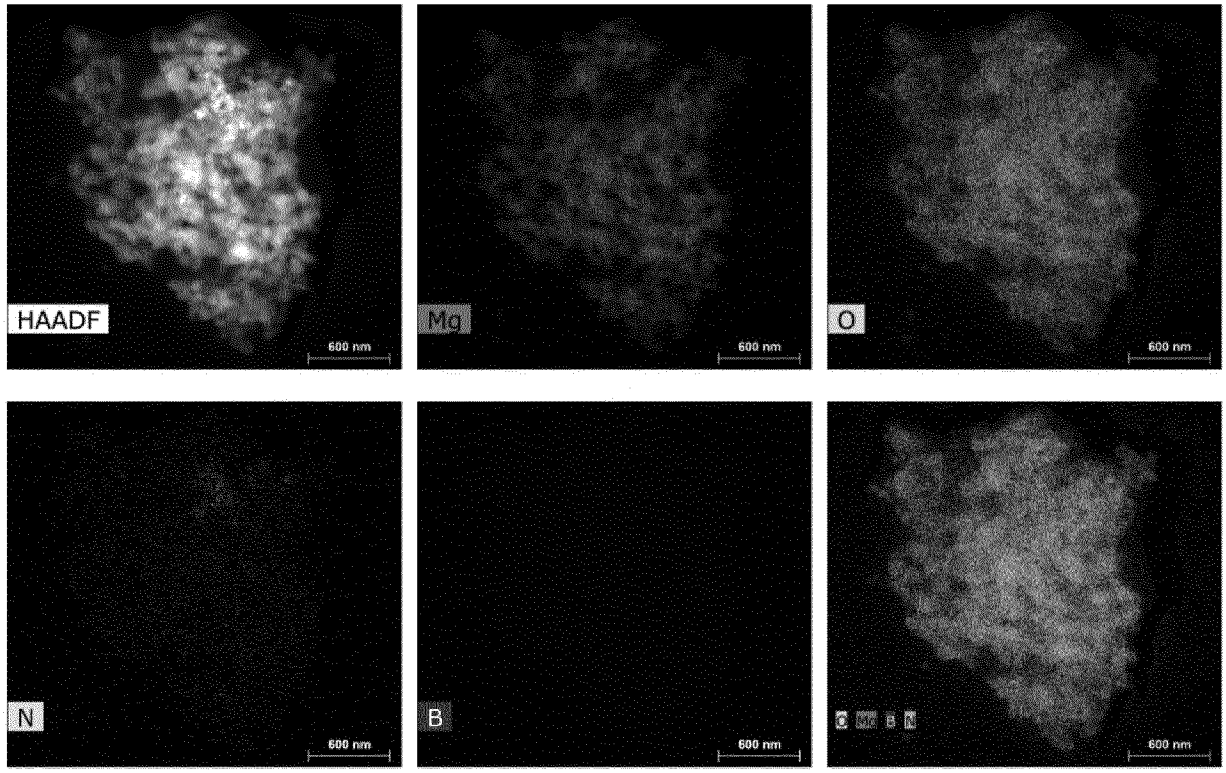
HAADF
Mg
O
N
B
600 nm

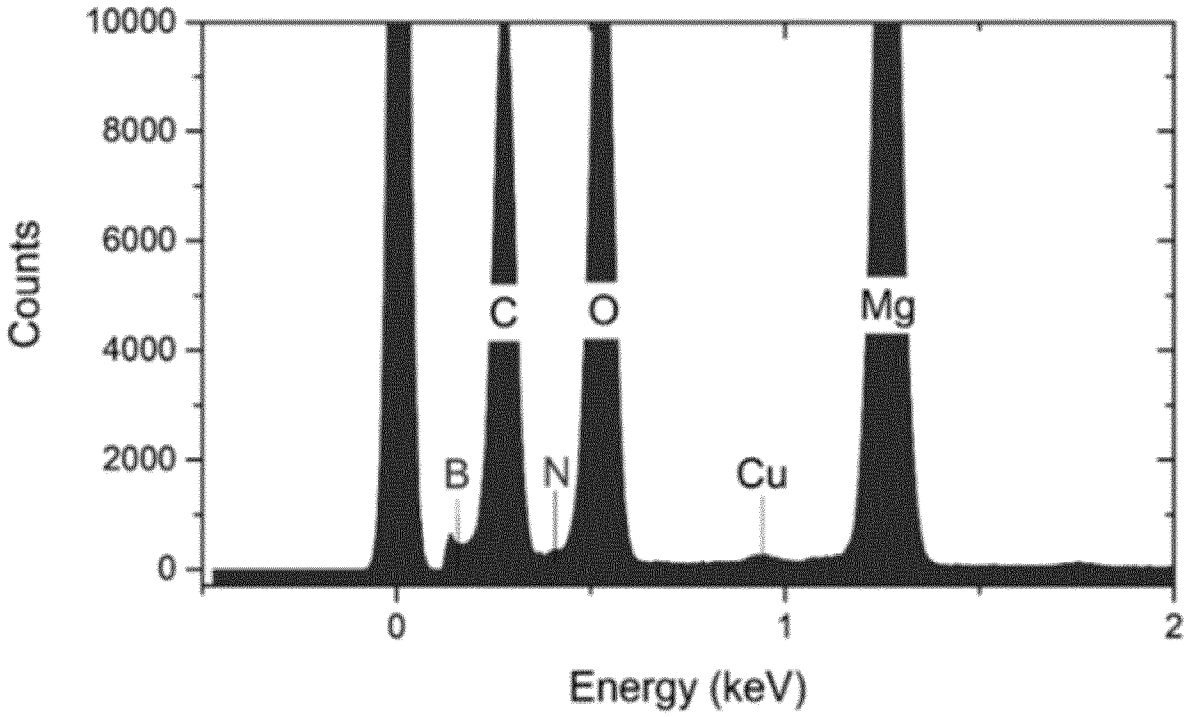
10000
8000
6000
4000
2000
0
Counts
C
O
Mg
B
N
Cu
0
1
2
Energy (keV)

FIG. 30

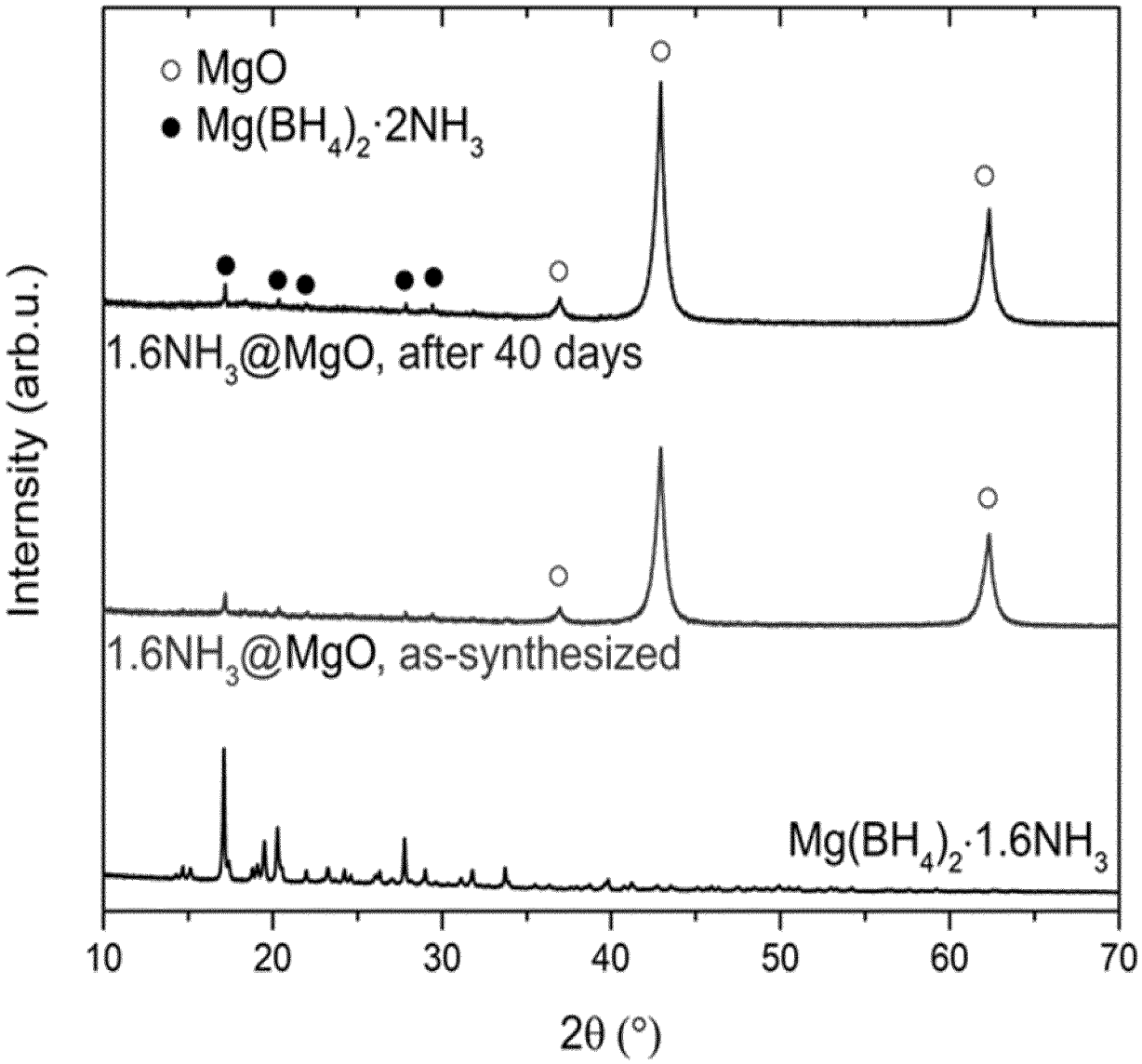
MgO
Mg(BH4)2·2NH3
1.6NH3@MgO, after 40 days
1.6NH3@MgO, as-synthesized
Mg(BH4)2·1.6NH3
Internsity (arb.u.)
10
20
30
40
50
60
70
2θ (°)

FIG. 31

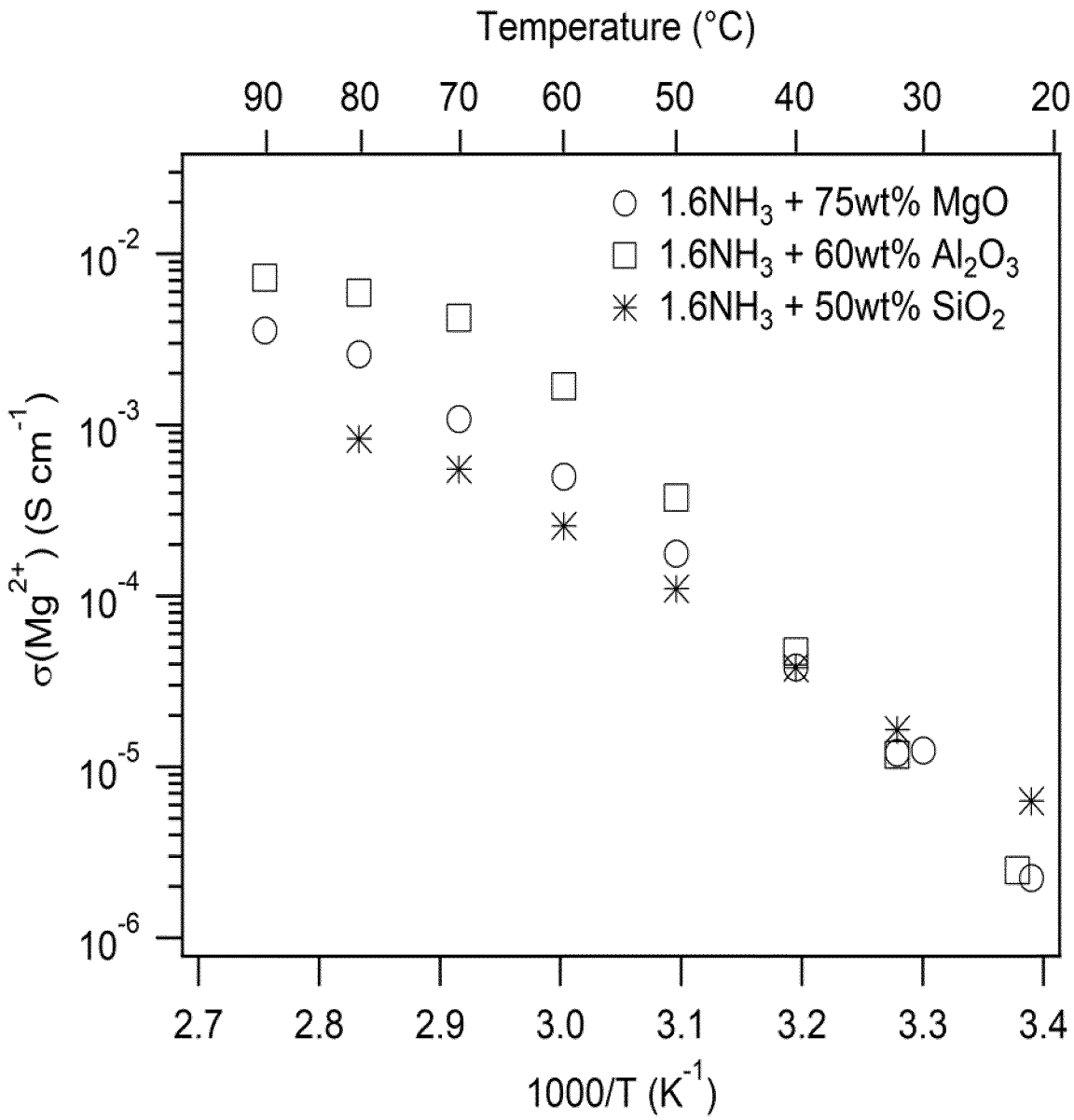
Temperature (°C)
90
80
70
60
50
40
30
20
1.6NH3 + 75wt% MgO
1.6NH3 + 60wt% Al2O3
1.6NH3 + 50wt% SiO2
σ(Mg2+) (S cm-1)
10-2
10-3
10-4
10-5
10-6
2.7
2.8
2.9
3.0
3.1
3.2
3.3
3.4
1000/T (K-1)

FIG. 32

FIG. 33

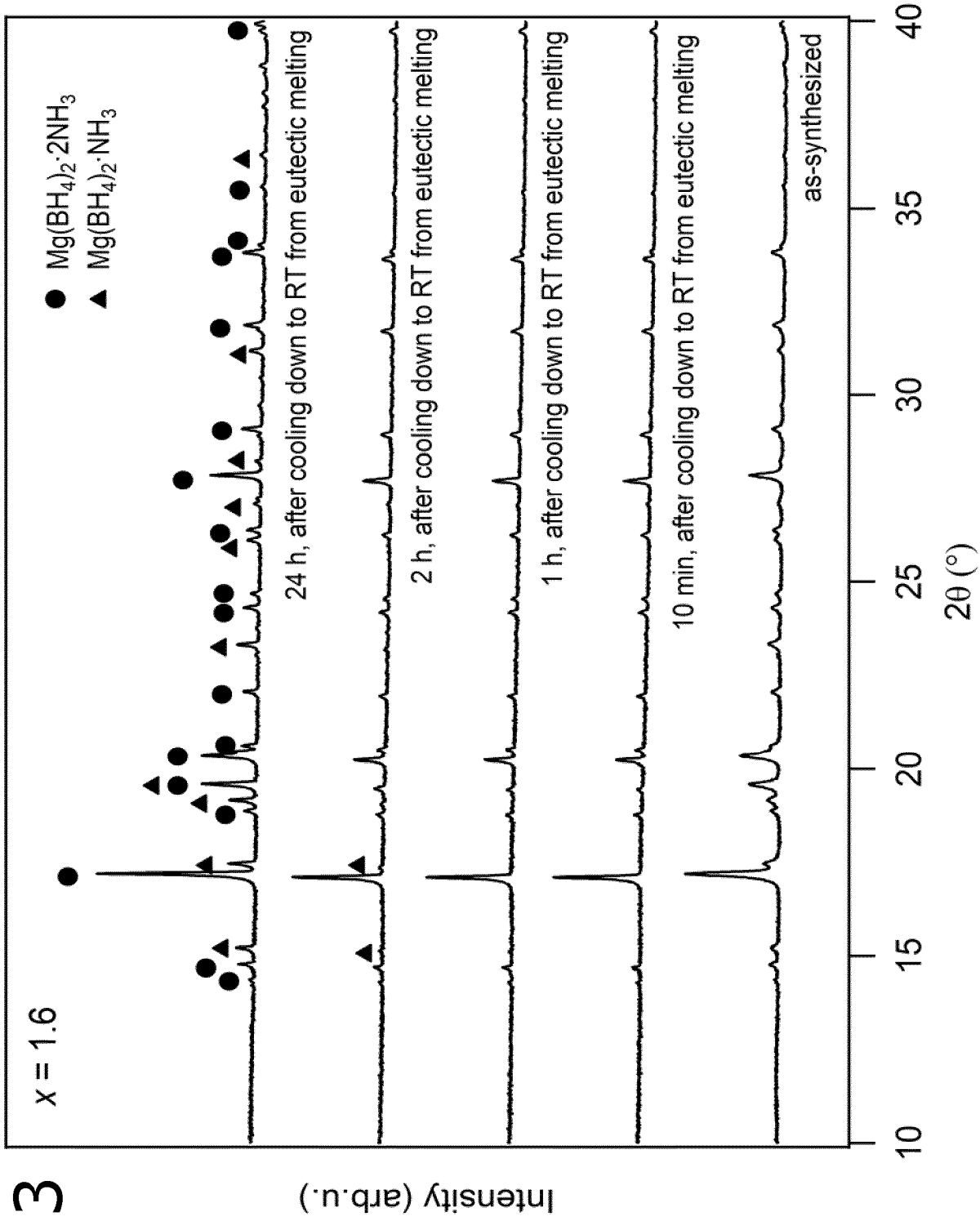
x = 1.6
Mg(BH4)2·2NH3
Mg(BH4)2·NH3
24 h, after cooling down to RT from eutectic melting
2 h, after cooling down to RT from eutectic melting
1 h, after cooling down to RT from eutectic melting
10 min, after cooling down to RT from eutectic melting
as-synthesized
Intensity (arb.u.)
10
15
20
25
30
35
40
2θ (°)

The ^{11}B MAS NMR data measured of the composite, $Mg(BH_4)_2 \cdot 1.6NH_3$, i.e. $0.4Mg(BH_4)_2 \cdot NH_3 – 0.6Mg(BH_4)_2 \cdot NH_3$, 10 min after melting the sample (heated to 70 °C for 15 min) show one sharp resonance at –40.4 ppm and two weak signals at –41.6 ppm and –42.2 ppm, the latter assigned to $Mg(BH_4)_2 \cdot 2NH_3$.

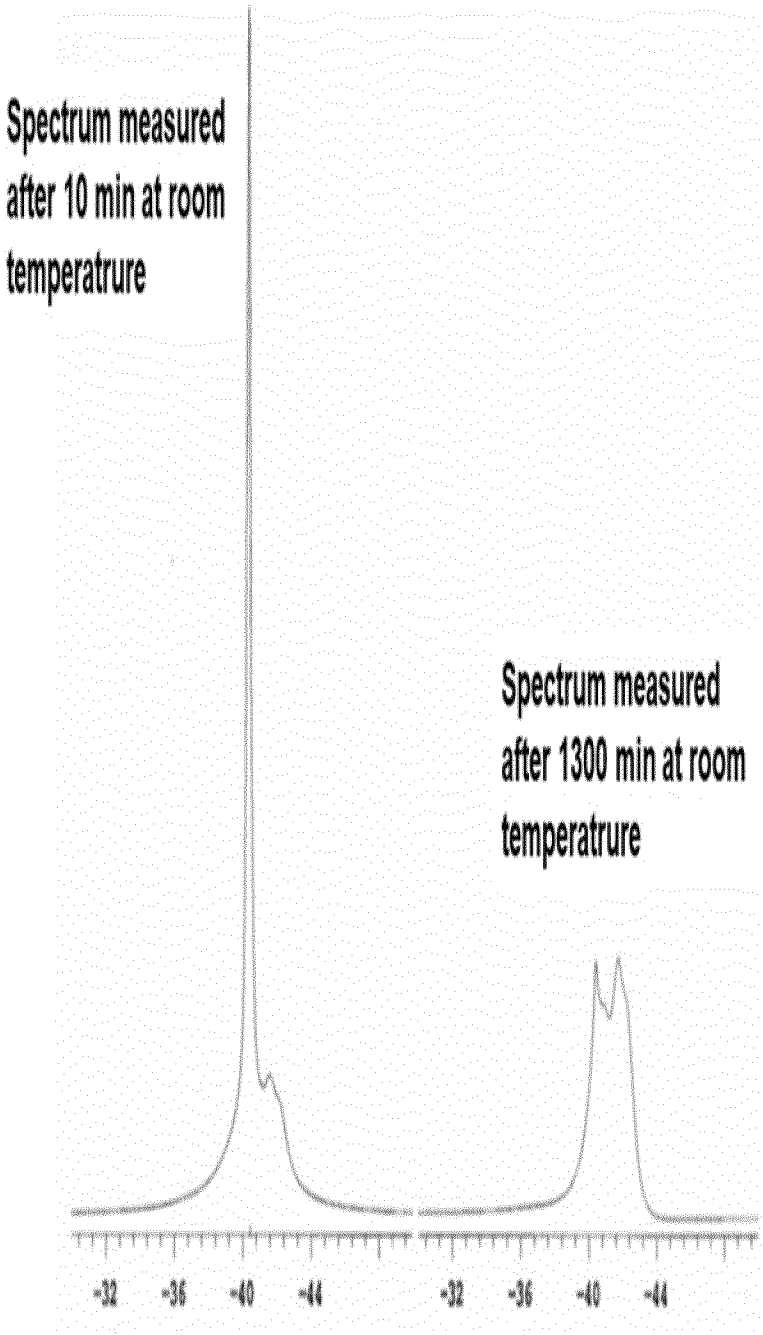

FIG. 34

INTERNATIONAL SEARCH REPORT

International application No
PCT/EP2019/074557

A. CLASSIFICATION OF SUBJECT MATTER
INV. H01M10/054 H01M10/0562
ADD.

According to International Patent Classification (IPC) or to both national classification and IPC

B. FIELDS SEARCHED

Minimum documentation searched (classification system followed by classification symbols)
H01M

Documentation searched other than minimum documentation to the extent that such documents are included in the fields searched

Electronic data base consulted during the international search (name of data base and, where practicable, search terms used)
EPO-Internal, WPI Data, CHEM ABS Data

C. DOCUMENTS CONSIDERED TO BE RELEVANT

Category*	Citation of document, with indication, where appropriate, of the relevant passages	Relevant to claim No.
A	CN 102 659 079 A (UNIV ZHEJIANG) 12 September 2012 (2012-09-12) cited in the application paragraphs [0012] - [0022], [0045] - [0056] -----	1-16
A	US 4 673 528 A (ARTZ GLEN D [US] ET AL) 16 June 1987 (1987-06-16) column 7, line 45 -----	1-16
A	US 2013/316249 A1 (HIGASHI SHOUGO [JP] ET AL) 28 November 2013 (2013-11-28) paragraph [0012] -----	1-15

☐ Further documents are listed in the continuation of Box C.

☒ See patent family annex.

* Special categories of cited documents :

"A" document defining the general state of the art which is not considered to be of particular relevance

"E" earlier application or patent but published on or after the international filing date

"L" document which may throw doubts on priority claim(s) or which is cited to establish the publication date of another citation or other special reason (as specified)

"O" document referring to an oral disclosure, use, exhibition or other means

"P" document published prior to the international filing date but later than the priority date claimed

"T" later document published after the international filing date or priority date and not in conflict with the application but cited to understand the principle or theory underlying the invention

"X" document of particular relevance; the claimed invention cannot be considered novel or cannot be considered to involve an inventive step when the document is taken alone

"Y" document of particular relevance; the claimed invention cannot be considered to involve an inventive step when the document is combined with one or more other such documents, such combination being obvious to a person skilled in the art

"&" document member of the same patent family

Date of the actual completion of the international search	Date of mailing of the international search report
29 October 2019	06/11/2019

Name and mailing address of the ISA/	Authorized officer
European Patent Office, P.B. 5818 Patentlaan 2 NL - 2280 HV Rijswijk Tel. (+31-70) 340-2040, Fax: (+31-70) 340-3016	Schwake, Andree

1

INTERNATIONAL SEARCH REPORT

Information on patent family members

International application No
PCT/EP2019/074557

Patent document cited in search report	Publication date	Patent family member(s)	Publication date
CN 102659079 A	12-09-2012	NONE	
US 4673528 A	16-06-1987	NONE	
US 2013316249 A1	28-11-2013	JP 5900144 B2	06-04-2016
		JP 2013239353 A	28-11-2013
		US 2013316249 A1	28-11-2013